

Critical Matter

Leo Radzihovsky

Department of Physics, University of Colorado, Boulder, CO 80309, USA

(Dated: June 7, 2023)

I review a class of novel ordered states of “critical matter”, that exhibit strongly fluctuating universal power-law orders, controlled by an infra-red attractive, non-Gaussian fixed point. I will illustrate how RG methods pioneered by Wilson and Fisher can be used to deduce critical phenomenology of such critical phases, resembling that of a critical point of second order phase transitions, but requiring no fine tuning.

I. INTRODUCTION

Michael Fisher is a towering figure in theoretical physics, most notably recognized for his seminal development (in collaboration with Ken Wilson and building on the works of Kadanoff, Migdal, Widom, Larkin, Pokrovsky, and others) of the renormalization group (RG)[1–3] and its numerous early applications to critical phenomena of continuous phase transitions[4]. In these works Michael transformed Wilson’s deep ideas[2, 3] into a practical and powerful theoretical tool for controlled calculations[1] (complementing more formal developments in quantum field theory[5]) and demonstrated its power through numerous seminal applications to critical phenomena. With this, he elevated RG into a central calculation tool in modern theoretical physics.

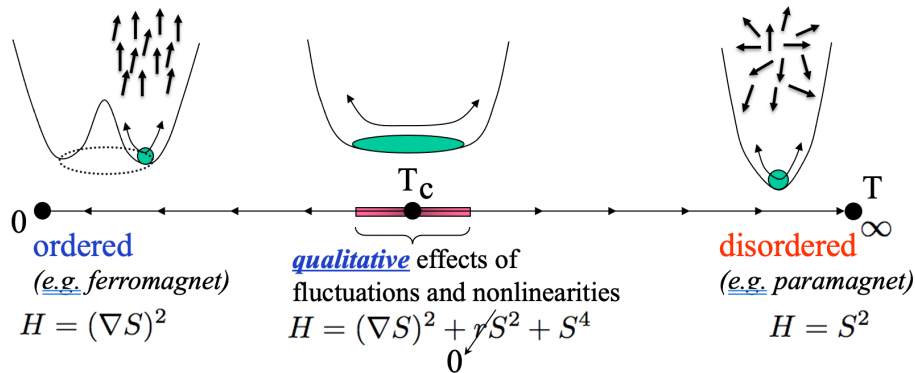


FIG. 1: Illustration of unimportance of fluctuations inside phases of conventional systems, where qualitative effects of thermal fluctuations are confined to a vicinity of a critical point.

Beginning with the earliest seminal analysis of the ϕ^4 field theory to describe criticality of the Ising paramagnet-ferromagnet transition, most applications of RG are used to treat enhanced fluctuations near a critical point of a continuous phase transition, where direct perturbation theory breaks down. In such applications a critical behavior emerges after tuning a set of parameters - e.g., temperature, pressure, magnetic field, etc, to a (multi-) critical point in a phase diagram, as illustrated in Fig.1. It is only then that fluctuations and nonlinearities (interactions) become important (below the upper-critical dimension) and universal asymptotic critical behavior emerges, e.g., power-law, scale-free correlation functions and thermodynamic responses with universal exponents[6].

In contrast to critical points, as illustrated in Fig.1 phases of matter, by their very definition are stable to weak generic perturbations that do not explicitly break their symmetry. They are thus characterized by infrared *attractive* fixed points, and thereby require no fine-tuning, in contrast to a critical point that separates them. Fluctuations in ordered Landau phases of matter[8] (that is our focus here) are characterized by their Goldstone modes associated with the spontaneous breaking of a *continuous* symmetry – Landau phases that break *discrete* symmetries have no interesting fluctuations. Despite being gapless, generically within ordered phases Goldstone-mode fluctuations are small, with finite root-mean-squared fluctuations, latter typically taken as the defining property of the ordered phase. In the RG parlance, this corresponds to typical phases that are controlled by a Gaussian attractive fixed point, as illustrated in Fig.1. Thus, conventional Landau phases’ description is effectively trivial, with fluctuations (above the lower-critical dimension, where the ordered phase is stable) only leading to small corrections to their mean-field description.

In this chapter I instead focus on an exotic class of ordered phases of matter – “critical phases”, e.g., smectics, cholesterics, columnar phases, membranes, elastomers, . . . , illustrated in Fig.2 – where in stark contrast to conventional phases, Goldstone-mode fluctuations are divergingly strong, interacting, and thus are controlled by a *non*-Gaussian infrared attractive fixed point, as illustrated in Fig.3. As such the resulting ordered critical phase, while breaking a

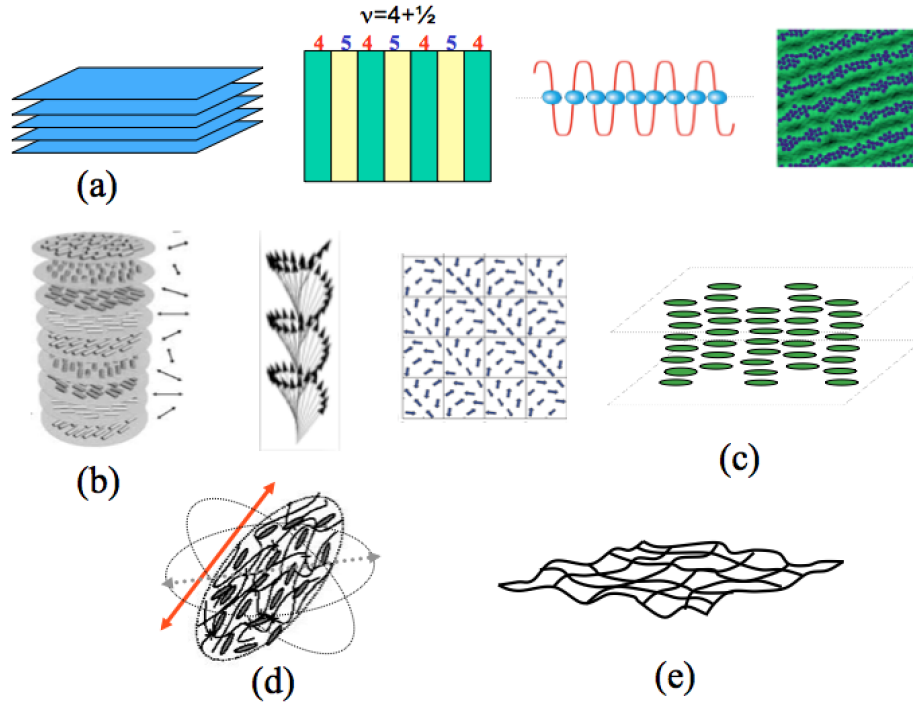


FIG. 2: Illustration of critical phases: (a) smectics realized as conventional liquid crystals[4, 10–14], 2d colloids[15], quantum-Hall systems[16–22] and as striped “pair-density wave” FFLO[23, 24] superconducting phases in degenerate atomic gases[25–27], p-wave resonant[28], spin-orbit coupled[29] and frustrated superfluids[30], (b) cholesteric liquid crystals[4, 10, 31, 32] and helical state of frustrated magnets[32–35], (c) columnar liquid crystals and spontaneous vortex lattices[36–41], (d) nematic elastomers[42, 43], and (e) polymerized membranes[44–49].

continuous symmetry is highly nontrivial and strongly interacting, with little resemblance of its mean-field cartoon. It is characterized by universal critical exponents, but in striking contrast to a critical point requires no fine-tuning, protected by underlying spontaneously broken symmetries, with importance of strong fluctuations and nonlinearities extending throughout the ordered phase. A generic ingredient of such critical phases (often associated with spontaneous breaking of *continuous* spatial symmetries) is that underlying symmetry enforces an exact *vanishing* of a subset of elastic moduli, resulting in particularly “soft” harmonic elasticity of the associated Goldstone modes, described by *m*-Lifshitz models[9, 50].

In subsequent sections of this chapter, I will illustrate above phenomenology through a set of examples of critical phases, some illustrated in Fig.2. I will begin with a detailed discussion of a quintessential critical phases – uniaxially periodically modulated states that spontaneously break translational and rotational symmetry, and are realized in numerous physical contexts, including smectic liquid crystals[4, 10, 11], cholesterics[32], helical magnets and bosons on frustrated lattices[30, 32–34], nonzero momentum superfluids such as Fulde-Ferrell-Larkin-Ovchinnikov (FFLO) superconductors[25, 26], p-wave resonantly paired bosons[28], spin-orbit coupled bosons[29], and quantum-Hall striped states[16–21]. In Sec. 3, I will describe a columnar states, that appear in discotic liquid crystals[4, 10, 39] and in its line-crystal analogs, such as putative spontaneous vortex lattice in magnetic superconductors[40, 41]. I will analyze another rich example of a critical phase – a thermally fluctuating tensionless polymerized membrane in Sec. 4.[44–48] In Sec. 5, I will discuss a nematic elastomer – a liquid crystal rubber, that, mathematically is a three-dimensional amalgam of a smectic and columnar phases, displaying critical phenomenology throughout its phase[42, 43].

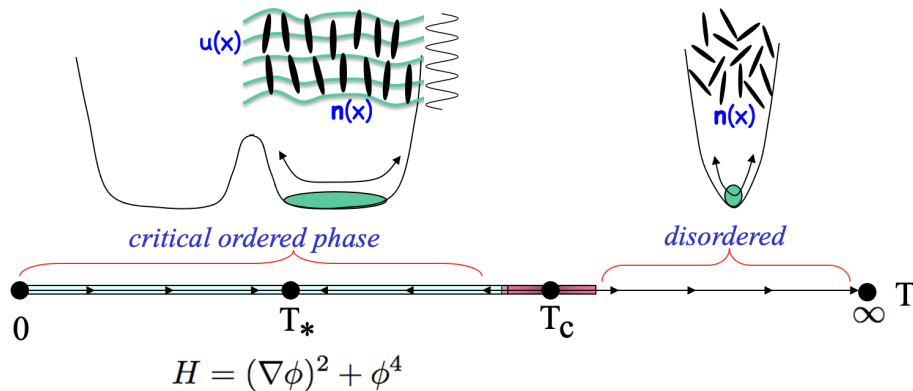


FIG. 3: Illustration of the importance of fluctuations inside ordered phases of “critical matter”, in which even deep in the ordered phase the quartic potential is missing the stabilizing quadratic contribution, resulting in divergent fluctuations akin to a critical point. The bottom of the figure is a schematic of a renormalization group flow, e.g., for a smectic state in $d < 3$ dimensions, illustrating that at low T it is a “critical phase” displaying universal power-law phenomenology, controlled by a nontrivial infrared-stable fixed point.

II. UNIAXIALLY PERIODIC CRITICAL STATES

There is a number of states of matter that *spontaneously* develop a periodic modulation along an arbitrarily chosen *single* axis. Strictly speaking this can only take place in a system with underlying rotational invariance, though can be exhibited over an extended intermediate regime when explicitly broken rotational symmetry couples only weakly, as e.g., in low density electronic systems.[16, 17]

Beyond conventional liquid crystals, some of the novel systems include helical states of frustrated and spin-orbit coupled magnets and bosons[29, 30, 33–35], and strongly correlated electronic and bosonic systems (quite surprising for isotropic and point constituents), such as FFLO[25] “striped” (“pair density wave”) superconductors[20, 27], finite momentum superfluids[28–30], and a two-dimensional electron gas in the quantum Hall regime of half-filled Landau level [16–22]. The underlying unifying feature of these diverse set of critical systems is the *spontaneously* broken rotational (in contrast to e.g., density waves in crystalline solids) and translational symmetries. Based on these symmetries that they break, we collectively refer to this class of states as smectics akin to their conventional soft matter liquid crystal realizations, that we turn to next.

A. Smectic liquid crystals

Illustrated in Fig.4, the most ubiquitous liquid crystal phases are the uniaxial nematic, that spontaneously breaks rotational symmetry of the parent isotropic fluid and the smectic state, a uniaxial one-dimensional density wave that further breaks translational symmetry along a single axis. The uniaxial nematic is characterized by a quadrupolar order parameter $Q_{ij} = S(\hat{n}_i \hat{n}_j - \frac{1}{3} \delta_{ij})$, with S the strength of the orientational order along the principle uniaxial axis $\hat{\mathbf{n}}$. A three-dimensional smectic-A is a periodic array of two-dimensional fluids, characterized by a uniaxial periodic density modulation with Fourier components that are integer multiples of the smectic ordering wavevector $\mathbf{q}_0 = \hat{\mathbf{n}} 2\pi/a$ (with a the layer spacing) parallel to the nematic director $\hat{\mathbf{n}}$; other type of smectics, e.g., smectic-C, where $\hat{\mathbf{n}}$ makes a nonzero angle with \mathbf{q}_0 are common.[4, 10] The dominant lowest Fourier component $\psi(\mathbf{x}) \equiv \rho_{\mathbf{q}_0}$ can be taken as the local (complex scalar) order parameter which distinguishes the smectic-A from the nematic phase[10]. It is related to the molecular density $\rho(\mathbf{x})$ by

$$\rho(\mathbf{x}) = \text{Re}[\rho_0 + \psi(\mathbf{x})e^{i\mathbf{q}_0 \cdot \mathbf{x}}], \quad (1)$$

where ρ_0 is the mean density of the smectic, $\psi = \rho_{\mathbf{q}_0}$ is the Fourier amplitude of the density at wavevector \mathbf{q}_0 and Re is a real part.

As first introduced by de Gennes[10], the effective Hamiltonian functional $H_{dG}[\psi, \hat{\mathbf{n}}]$, that describes the nematic-to-smectic-A (NA) transition at long length scales, is given by,

$$H_{dG}[\psi, \hat{\mathbf{n}}] = \int d^d x \left[c |(\nabla - iq_0 \delta \hat{\mathbf{n}})\psi|^2 + t_0 |\psi|^2 + \frac{1}{2} g_0 |\psi|^4 \right] + H_F[\mathbf{n}], \quad (2)$$

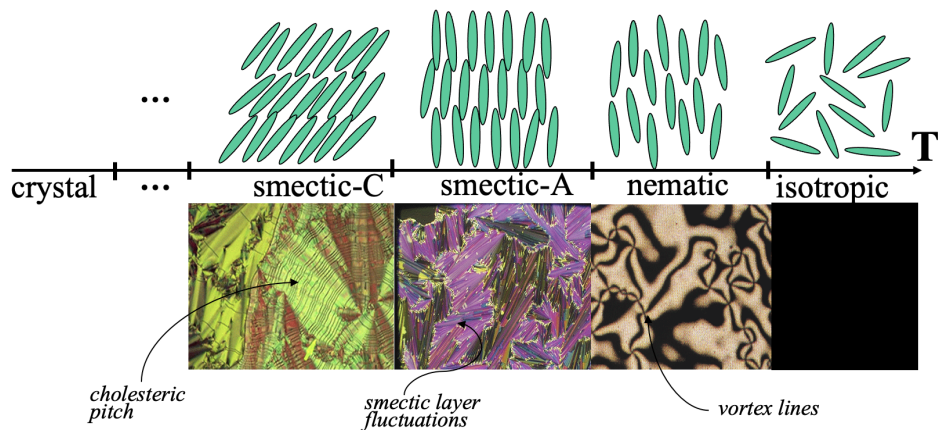


FIG. 4: Illustration of the most ubiquitous nematic (orientationally ordered uniaxial fluid), smectic-A and smectic-C (one-dimensional density wave with, respectively isotropic and polar in-plane fluid orders) liquid crystal phases and their associated textures in cross-polarized microscopy (N.A. Clark laboratory).

where $t_0 \propto T - T_{NA}$ is the reduced temperature for transition at T_{NA} ,

$$\delta \hat{\mathbf{n}}(\mathbf{x}) \equiv \hat{\mathbf{n}}(\mathbf{x}) - \hat{\mathbf{n}}_0 = \delta \hat{\mathbf{n}}_{\perp} + \hat{\mathbf{n}}_0 (\sqrt{1 - \delta \hat{\mathbf{n}}_{\perp}^2} - 1) \quad (3)$$

is the fluctuation of the local nematic director $\hat{\mathbf{n}}(\mathbf{x})$ away from its average value $\hat{\mathbf{n}}_0$, which I take to be $\hat{\mathbf{z}}$, and $H_F[\hat{\mathbf{n}}]$ is the Frank effective Hamiltonian that describes the elasticity of the nematic director:

$$H_F[\hat{\mathbf{n}}] = \int d^d x \frac{1}{2} \left[K_s (\nabla \cdot \hat{\mathbf{n}})^2 + K_t (\hat{\mathbf{n}} \cdot \nabla \times \hat{\mathbf{n}})^2 + K_b (\hat{\mathbf{n}} \times \nabla \times \hat{\mathbf{n}})^2 \right], \quad (4)$$

where K_s , K_t , and K_b are the bare elastic moduli for splay, twist and bend of the nematic director field, respectively.[4, 10]

The “minimal” gauge-like coupling between \mathbf{n} and ψ is enforced by the requirement of global rotational invariance[10]. It is important to emphasize, however, that although de Gennes Hamiltonian H_{dG} closely resembles the Ginzburg-Landau model of a superconductor and the Abelian-Higgs model, there are essential differences, that are discussed in the chapter by Tom Lubensky. The physical reality of the nematic director $\hat{\mathbf{n}}$ and the smectic order parameter ψ (in contrast to the gauge ambiguity in the definition of the vector potential and the superconducting order parameter), selects the liquid crystal gauge $\delta \hat{\mathbf{n}}_{\perp} \cdot \hat{\mathbf{n}}_0 = 0$ as the physical gauge in which $\hat{\mathbf{n}}$ and ψ are measured. The strict gauge invariance is also explicitly broken in H_{dG} by the splay term $K_s (\nabla \cdot \hat{\mathbf{n}})^2$ of the Frank Hamiltonian (contrasting with the Maxwell action that involves purely gauge invariant derivatives, e.g., $(\nabla \times \mathbf{A})^2$), that, as we will see below determines the smectic Goldstone-mode elasticity.

B. Smectic elasticity

1. Smectic from a nematic liquid crystal fluid

Within the ordered smectic phase, the fluctuations are conveniently described in terms of the magnitude and phase of the smectic order parameter ψ . It is easy to show that the fluctuations of the *magnitude* of ψ around the average value $|\psi_0| = \sqrt{t_0/g_0} = \text{const.}$ are “massive”, and can therefore be safely integrated out of the partition function, leading to only *finite*, unimportant shifts in the effective elastic moduli. In contrast, the phase of ψ is a U(1) massless Goldstone mode, corresponding to spontaneously broken translational symmetry along \mathbf{q}_0 . It is the low-energy phonon degree of freedom of the smectic state, describing local displacement of the smectic layers from its perfect periodic order. In accord with this discussion, deep within the smectic phase, we can represent the smectic order parameter as

$$\psi(\mathbf{x}) = |\psi_0| e^{-iq_0 u(\mathbf{x})}, \quad (5)$$

safely neglecting fluctuations in the magnitude $|\psi_0|$ at temperature below the T_{NA} .

Using this low-temperature smectic description (5) inside the de Gennes Hamiltonian (2) and dropping constants, one finds

$$H[u, \delta \hat{\mathbf{n}}_{\perp}] = \int d^d x \left[\frac{B}{2} (\nabla_{\perp} u + \delta \hat{\mathbf{n}}_{\perp})^2 + \frac{B}{2} (\partial_z u - \frac{1}{2} \delta \hat{n}_{\perp}^2)^2 + \frac{K_s}{2} (\nabla \cdot \delta \hat{\mathbf{n}})^2 + \frac{K_t}{2} (\hat{\mathbf{z}} \cdot \nabla \times \delta \hat{\mathbf{n}})^2 + \frac{K_b}{2} (\hat{\mathbf{z}} \times \nabla \times \delta \hat{\mathbf{n}})^2 \right], \quad (6)$$

where $B = 2c|\psi_0|^2 q_0^2$ is the smectic compression modulus. I observe that the fluctuation mode $\nabla_{\perp} u + \delta \hat{\mathbf{n}}_{\perp}$ is “massive” and leads to an emergent Anderson-Higgs-like mechanism, a hallmark of gauge theories. As a consequence, after a simple Gaussian integration over $\delta \hat{\mathbf{n}}_{\perp}$, one finds that at long length scales, $\delta \hat{\mathbf{n}}_{\perp}$ fluctuations are constrained to follow $\nabla_{\perp} u$, corresponding to locking of the director $\hat{\mathbf{n}}$ to the smectic layer normal. The low-energy elastic smectic Hamiltonian is then obtained by the replacement

$$\delta \hat{\mathbf{n}}_{\perp} \rightarrow -\nabla_{\perp} u, \quad (7)$$

everywhere in Eq.(6) and Frank energy Eq.(4). Valid in the long wavelength limit and provided dislocations are confined, one thus obtain a nonlinear elastic Goldstone-mode Hamiltonian of the smectic phase,

$$H_{sm}[u] = \int d^d x \left[\frac{K}{2} (\nabla_{\perp}^2 u)^2 + \frac{B}{2} (\partial_z u - \frac{1}{2} (\nabla u)^2)^2 \right], \quad (8)$$

where $K = K_s$ is the splay modulus.[4, 11]

I observe that the harmonic elasticity of the smectic – $m = d-1$ -Lifshitz model[9] – is highly anisotropic (at harmonic level with scaling $z \sim x_{\perp}^2$), displaying compression modulus B along \mathbf{q}_0 and higher-order *curvature* (Laplacian) modulus transverse to \mathbf{q}_0 , with the “tension” (transverse gradient) modulus vanishing exactly. This is ensured by the underlying rotational symmetry, as discussed in the Introduction to critical phases. As I will show in forthcoming sections, as a consequence, smectic fluctuations are highly enhanced (relative to e.g., its XY model counterpart), resulting in importance of nonlinear Goldstone-modes’ elasticity for $d \leq 3$, that I therefore retained in (8). I also note that the compressional modulus B multiplies a square of the nonlinear strain tensor, whose precise form is determined by the underlying invariance under arbitrary large rotation of smectic layers,

$$u_0(\mathbf{r}) = z(1 - \cos \theta) + x \sin \theta, \quad (9)$$

and maintained under coarse-graining RG. I conclude this subsection by also noting that the aforementioned connection to the Anderson-Higgs mechanism elucidates why a smectic state is characterized by only a single Goldstone mode u , rather than three, despite partially breaking two rotational and one translational symmetries. In contrast, a charged superconductor is well-known to have all its Goldstone modes “eaten” – fully gapped out by the Anderson-Higgs mechanism.

2. Smectic from an isotropic fluid

I now derive the nonlinear smectic elasticity in a more basic, complementary way, starting instead with an isotropic fluid state.[11] I begin with a generic energy functional that captures system’s tendency to develop a unidirectional wave at wavevector \mathbf{q}_0 , with an arbitrary direction, and magnitude fixed at q_0 ,

$$\mathcal{H}_{sm} = \frac{1}{2} J [(\nabla^2 \rho)^2 - 2q_0^2 (\nabla \rho)^2] + \frac{1}{2} t \rho^2 - w \rho^3 + v \rho^4 + \dots, \quad (10)$$

where J, q_0, t, w, v are parameters of the isotropic fluid phase. Clearly, the first term is engineered so that dominant fluctuations and condensation are on a spherical surface at a nonzero wavevector with a magnitude q_0 . Thus I focus on the density at a wavevector \mathbf{q} , that for now is unrelated to q_0

$$\rho(\mathbf{x}) = \text{Re} [\rho_q(\mathbf{x}) e^{i\mathbf{q} \cdot \mathbf{x}}], \quad (11)$$

where $\rho_q(\mathbf{x})$ is a complex scalar. Without loss of generality, based on the discussion of the previous subsection, the order parameter $\rho_q(\mathbf{x}) = |\rho_q| e^{-iq u}$ is taken to have a (constant) magnitude $|\rho_q|$ and a phase $qu(\mathbf{x})$. Clearly $u(\mathbf{x})$ is just a phonon displacement along \mathbf{q} . Substituting this expression for $\rho(\mathbf{x})$ and its gradients into \mathcal{H}_{sm} one finds

$$\mathcal{H}_{sm} = J \rho_0^2 \left[\frac{1}{4} q^2 (\nabla^2 u)^2 + \left(\mathbf{q} \mathbf{q} \cdot \nabla u - \frac{1}{2} q^2 (\nabla u)^2 \right)^2 + 4(q^2 - q_0^2) \left(\mathbf{q} \mathbf{q} \cdot \nabla u - \frac{1}{2} q^2 (\nabla u)^2 \right) \right] + \dots, \quad (12)$$

where constant parts as well as fast oscillating pieces were dropped as they average away after spatial integration of the above energy density. Firstly, I observe that (as discussed on general grounds above) in a harmonic part linear gradient elasticity in u only appears for gradients *along* \mathbf{q} , namely $\mathbf{q} \cdot \nabla$, with elasticity transverse to \mathbf{q} starting with a Laplacian form. Secondly, the elastic energy density is an expansion in a rotationally-invariant strain tensor combination

$$u_{qq} = \hat{\mathbf{q}} \cdot \nabla u - \frac{1}{2}(\nabla u)^2, \quad (13)$$

whose nonlinearities in u ensure that it is fully rotationally invariant even for large rotations. To see this (picking $\hat{\mathbf{q}} = \hat{\mathbf{z}}$) note that a rigid (distortion-free) rotation of \mathbf{q} ($q_0 \hat{\mathbf{z}} \rightarrow \mathbf{q} = q_0(\cos \theta \hat{\mathbf{z}} + \sin \theta \hat{\mathbf{x}}$), can be interpreted as a spatially linear “distortion” $u_0(\mathbf{x}) = z(1 - \cos \theta) + x \sin \theta$, for which nonlinear strain u_{qq} vanishes identically, thus, as required, corresponds to a vanishing energy. Thirdly, the last term in (12) vanishes for $|\mathbf{q}|$ picked to equal q_0 , corresponding to energetically preferred choice of modulation wavevector.

Looking ahead, as one includes effects of fluctuations, the “bare” condition $q = q_0$ will need to be adjusted so as to eliminate the fluctuation-generated linear term in u_{qq} order by order, which amounts to an expansion in the nonlinear strain u_{qq} around the correct (fluctuation-corrected) ground state. Finally, I note that the relation between the curvature modulus K of Laplacian (first) term and the bulk modulus B gradient (second) term is not generic and can be relaxed to have distinct elastic constants, as can be seen if higher order gradient terms are included in the original energy density, Eq. (10).

Choosing the coordinate system such that $\hat{\mathbf{z}}$ is aligned along \mathbf{q} , one finds that for $q = q_0$, the Goldstone-mode Hamiltonian (12) reduces to the standard smectic elastic energy density, (8) derived from the de Gennes model above. [4, 10].

3. Smectic as cholesteric and helical fluids

Another beautiful example of a system that realizes a uniaxial periodic critical state is a cholesteric phase of chiral liquid crystals, illustrated in Fig.2(b). It is in fact the first liquid crystal phase discovered in cholesterol benzoate by Reinitzer in 1886.[4, 10] Such orientational (as opposed to mass) density wave state is ubiquitous in nature and is equivalent to the helical co-planar spin-spiral state that is found in non-centrosymmetric magnets like MnSi, FeSi and many others[33] (neglecting crystal-field pinning that is always present due to spin-orbit interactions and explicit breaking of rotational symmetry.).

Following analysis of Radzihovsky and Lubensky[32], below I discuss the low-energy *nonlinear* elasticity of a cholesteric, on length scales longer than its period, $a = 2\pi/q_0$. As first proposed by de Gennes, the latter is expected, based on symmetry and an explicit *harmonic* derivation by Lubensky[10, 31], to be identical to that of a smectic, i.e., that of a one-dimensional crystalline order, that spontaneously breaks underlying translational and rotational symmetry, with constant-orientation “layers” transverse to the ordering wavevector, \mathbf{q}_0 . Although the underlying chirality has only subtle surface effects within the cholesteric state, its effects become important in the nature of the phase transition in and out of the cholesteric critical state.

The simplest model of a chiral nematic liquid crystal (a cholesteric), is captured by the chiral Frank elastic free energy density,

$$\mathcal{H}_F^* = \frac{1}{2}K_s(\nabla \cdot \hat{n})^2 + \frac{1}{2}K_b(\hat{n} \times \nabla \times \hat{n})^2 + \frac{1}{2}K_t(\hat{n} \cdot \nabla \times \hat{n} + q_0)^2. \quad (14)$$

The broken chiral symmetry allows a chiral q_0 term, that leads to a twist of the nematic structure into a helix with a pitch $2\pi/q_0$ along a spontaneously chosen axis.

In a simplified isotropic limit of $K_s = K_b = K_t$, the chiral Frank energy density is then given by

$$\mathcal{H}_F^* = \frac{1}{2}K [(\partial_i \hat{n}_j)^2 + 2q_0 \hat{n} \cdot \nabla \times \hat{n} + q_0^2], \quad (15)$$

$$= \frac{1}{2}K (\partial_i \hat{n}_j + q_0 \epsilon_{ijk} \hat{n}_k)^2 - \frac{1}{2}K q_0^2, \quad (16)$$

where after integration by parts I utilized the identity

$$(\partial_i \hat{n}_j)^2 = (\nabla \cdot \hat{n})^2 + (\nabla \times \hat{n})^2 + \nabla \cdot [(\hat{n} \cdot \nabla) \hat{n} - \hat{n} \nabla \cdot \hat{n}]. \quad (17)$$

In the absence of topological defects, neglecting the boundary term, \mathcal{H}_F^* is a sum of squares and is therefore minimized by a twist-only cholesteric state

$$\hat{n}(\mathbf{r}) = \hat{\mathbf{e}}_{10} \cos(\mathbf{q} \cdot \mathbf{r}) + \hat{\mathbf{e}}_{20} \sin(\mathbf{q} \cdot \mathbf{r}), \quad (18)$$

where $\hat{\mathbf{e}}_{10}, \hat{\mathbf{e}}_{20}, \hat{\mathbf{e}}_{30} \equiv \hat{\mathbf{e}}_{10} \times \hat{\mathbf{e}}_{20}$ form an orthonormal triad, with a constant twist

$$\hat{\mathbf{n}} \cdot \nabla \times \hat{\mathbf{n}} = -q_0. \quad (19)$$

I now derive the low-energy Goldstone-mode elasticity about the cholesteric helical ground state, that can be parameterized according to

$$\hat{\mathbf{n}}(\mathbf{r}) = \hat{\mathbf{e}}_1(\mathbf{r}) \cos(\mathbf{q} \cdot \mathbf{r} + \chi(\mathbf{r})) + \hat{\mathbf{e}}_2(\mathbf{r}) \sin(\mathbf{q} \cdot \mathbf{r} + \chi(\mathbf{r})), \quad (20)$$

where fluctuations are captured by the spatially dependent orthonormal triad $\hat{\mathbf{e}}_1(\mathbf{r}), \hat{\mathbf{e}}_2(\mathbf{r}), \hat{\mathbf{e}}_3(\mathbf{r})$ and the helical phase

$$\chi(\mathbf{r}) = -q_0 u(\mathbf{r}), \quad (21)$$

that corresponds to the phonon field $u(\mathbf{r})$ of the constant-orientation layers.

The helical state breaks a group of three dimensional translations and rotations $G = T_{x,y,z} \times O(3)$ of the isotropic fluid down to $H = T_x \times T_y \times U(1)$ (latter $U(1) = \text{diagonal}[T_z, O_z(2)]$). Thus, since $\dim[G/H = O(3)] = 3$, one may expect *three independent* Goldstone modes $\chi(\mathbf{r})$ and $\hat{\mathbf{e}}_3(\mathbf{r})$, corresponding to three degrees of freedom of the orthonormal triad; the azimuthal angle $\phi(\mathbf{r})$ defining the orientation of the $\hat{\mathbf{e}}_{1,2}$ around $\hat{\mathbf{e}}_3$ is not independent of $\chi(\mathbf{r})$ as it can be absorbed into it. The low-energy coset space is isomorphic to $S^1 \times S^2$, a ball (radius π) of the group manifold of $SO(3)$. However, despite of this standard counting, as I will show below and is expected on general grounds anticipated by de Gennes, the cholesteric state is characterized by a *single* smectic-like Goldstone mode $u(\mathbf{r})$.

To this end, substituting the form for $\hat{\mathbf{n}}(\mathbf{r})$ from Eq. (20) into the Frank energy of the chiral nematic (14), and defining effective connection gauge fields, \mathbf{a} and $\mathbf{c}_{1,2}$

$$\partial_i \hat{\mathbf{e}}_{1j} = a_i \hat{\mathbf{e}}_{2j} + c_{1i} \hat{\mathbf{e}}_{3j}, \quad (22a)$$

$$\partial_i \hat{\mathbf{e}}_{2j} = -a_i \hat{\mathbf{e}}_{1j} + c_{2i} \hat{\mathbf{e}}_{3j}, \quad (22b)$$

$$a_i = \hat{\mathbf{e}}_2 \cdot \partial_i \hat{\mathbf{e}}_1, \quad c_{1i} = -\hat{\mathbf{e}}_1 \cdot \partial_i \hat{\mathbf{e}}_3, \quad c_{2i} = -\hat{\mathbf{e}}_2 \cdot \partial_i \hat{\mathbf{e}}_3, \quad (22c)$$

one finds,

$$\mathcal{H}_F^* = \frac{K}{2} (\nabla \chi + \mathbf{a} + \mathbf{q} - q_0 \hat{\mathbf{e}}_3)^2 + \frac{K}{4} (\mathbf{c}_1 + q_0 \hat{\mathbf{e}}_2)^2 + \frac{K}{4} (\mathbf{c}_2 - q_0 \hat{\mathbf{e}}_1)^2. \quad (23)$$

In above, I again neglected spatially oscillating and constant terms.

Taking $\mathbf{q} = q_0 \hat{\mathbf{z}}$, with $\hat{\mathbf{z}}$ defining the helical axis (distinct from the normal to the helical plane, $\hat{\mathbf{e}}_3$) and noting the compatibility condition on effective flux or its equivalent vanishing of the Pontryagin density

$$\nabla \times \mathbf{a} = \epsilon_{ij} \hat{\mathbf{e}}_3 \cdot \partial_i \hat{\mathbf{e}}_3 \times \partial_j \hat{\mathbf{e}}_3 = 0, \quad (24)$$

required by well-defined cholesteric layers, i.e., in the absence of dislocations and disclinations in the layer structure, allows one to take

$$\mathbf{a} = \nabla \phi. \quad (25)$$

Under this condition ϕ can be eliminated in favor of χ , i.e., $\chi + \phi \rightarrow \chi$ and in the laboratory coordinate system $\hat{\mathbf{x}}, \hat{\mathbf{y}}, \hat{\mathbf{z}}$, the fluctuations are characterized by the local helical frame described by χ and $\hat{\mathbf{e}}_3$, with

$$\hat{\mathbf{e}}_3 = \hat{\mathbf{e}}_{3\perp} + \hat{\mathbf{z}} \sqrt{1 - \hat{\mathbf{e}}_{3\perp}^2} \approx \hat{\mathbf{e}}_{3\perp} + \hat{\mathbf{z}} (1 - \frac{1}{2} \hat{\mathbf{e}}_{3\perp}^2). \quad (26)$$

I thus obtain

$$\mathcal{H}_F^* = \frac{1}{2} (\nabla_{\perp} \chi - q_0 \hat{\mathbf{e}}_{3\perp})^2 + \frac{1}{2} (\partial_z \chi + \frac{1}{2} q_0 \hat{\mathbf{e}}_{3\perp}^2)^2 + \frac{1}{4} (\mathbf{c}_1^2 + \mathbf{c}_2^2) + \frac{q_0}{2} (\mathbf{c}_1 \cdot \hat{\mathbf{e}}_2 - \mathbf{c}_2 \cdot \hat{\mathbf{e}}_1). \quad (27)$$

From the minimization of the first term (or equivalently integrating out the independent $\hat{\mathbf{e}}_{3\perp}$ degree of freedom), I obtain an effective constraint

$$\nabla_{\perp} \chi = q_0 \hat{\mathbf{e}}_{3\perp}, \quad (28)$$

that is an example of an emergent Higgs mechanism (akin to smectic liquid crystals discussed above) locking the cholesteric layers with the molecular frame orientation. With this constraint (valid at low energies) the effective cholesteric Hamiltonian reduces to

$$\mathcal{H}_F^* = \frac{1}{2} [\partial_z \chi + \frac{1}{2q_0} (\nabla_{\perp} \chi)^2]^2 + \frac{1}{4q_0^2} (\hat{\mathbf{e}}_{\alpha\gamma} \cdot \partial_{\beta}^{\perp} \partial_{\gamma}^{\perp} \chi)^2 + \frac{q_0}{2} (\hat{\mathbf{e}}_{1\alpha} \hat{\mathbf{e}}_{2\beta} \partial_{\beta} \partial_{\alpha} \chi - \hat{\mathbf{e}}_{2\alpha} \hat{\mathbf{e}}_{1\beta} \partial_{\beta} \partial_{\alpha} \chi), \quad (29a)$$

$$= \frac{B}{2} [\partial_z u - \frac{1}{2} (\nabla u)^2]^2 + \frac{K}{2} (\nabla^2 u)^2 \quad (29b)$$

where compressional modulus $B = Kq_0^2$, $\hat{\mathbf{e}}_{\alpha,i}\hat{\mathbf{e}}_{\alpha,j} = \delta_{ij}$ and $\hat{\mathbf{e}}_{1,i}\hat{\mathbf{e}}_{2,j} - \hat{\mathbf{e}}_{2,i}\hat{\mathbf{e}}_{1,j} = \hat{\mathbf{e}}_{3,k}\epsilon_{ijk}$ were used, and to eliminate the last term in the first line above I used the condition of the single-valuedness of the phase field χ , i.e., well defined cholesteric layers with no dislocations. However, this last condition is violated and thus distinguishes the cholesteric from a smectic near a phase transition out of the cholesteric state.

Thus, as advertised and expected on symmetry grounds one indeed finds[32], that cholesteric Goldstone-mode elasticity, even at the nonlinear level is identical to that of a conventional smectic – at harmonic level controlled by the $m = d - 1$ -Lifshitz model[9]. Thus smectic critical state universal phenomenology, to be worked out below, will equally apply to the cholesteric state.

4. Smectic as a helical bosonic superfluid

I next discuss a quantum realization of a smectic state, namely via interacting superfluid bosons on a frustrated honeycomb lattice.[30] Other bosonic realizations also appear in p-wave Feshbach-resonant[28] and Rashba spin-orbital coupled [29] bosons, engineered in a controlled way in cold atom experiments[29, 51] to condense at a nonzero momentum, \mathbf{k}_0 .

I refer the reader to the original literature for these latter systems and here focus on bosons on a frustrated honeycomb lattice, modeled by a tight-binding dispersion with nearest t_1 and next-nearest (antiferromagnetic) $-t_2$ neighbor hopping amplitudes, with

$$H = -t_1 \sum_{\langle ij \rangle} a_{i,1}^\dagger a_{j,2} + t_2 \sum_{\langle\langle ij \rangle\rangle} (a_{i,1}^\dagger a_{j,1} + a_{i,2}^\dagger a_{j,2}) + h.c. + \frac{U}{2} \sum_i \sum_{s=1,2} n_{i,s}(n_{i,s} - 1). \quad (30)$$

For sufficiently frustrated hopping, with $t_2/t_1 > 1/6$ (that has been engineered in an optical lattice through Floquet techniques [51]), above system displays a dispersion minimum at a nonzero momentum closed contour, illustrated in Fig.5.

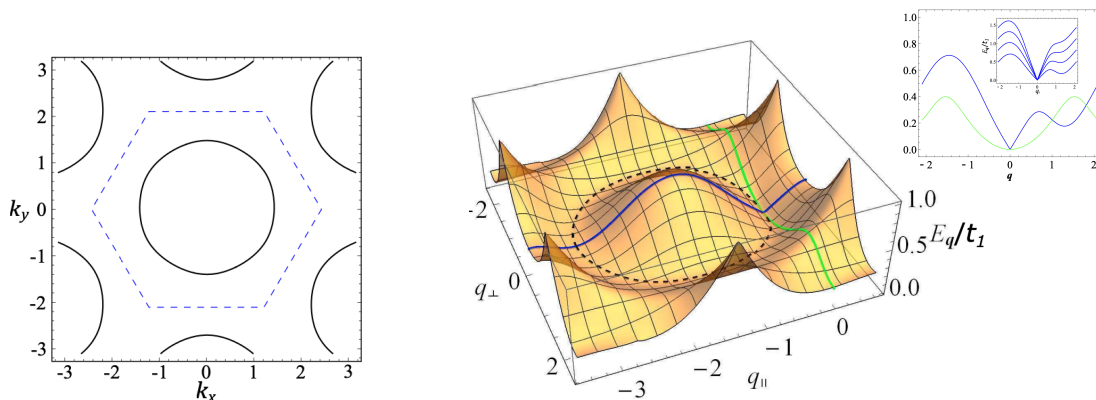


FIG. 5: (a) A black circular curve is a nonzero momentum \mathbf{k}_0 minimum in the noninteracting microscopic dispersion $\epsilon_{\mathbf{k}}^-$ (around the Γ point in the Brillouin zone, dashed blue curve) of bosons on a frustrated honeycomb lattice, (30). (b) The dispersion of the interacting helical superfluid, $E_{\mathbf{q}}$ around $\mathbf{q} = \mathbf{k} - \mathbf{k}_0 = 0$, with green (see inset) indicating quadratic q_{\perp}^2 form along q_{\perp} and blue (see inset) $|q_{\parallel}|$ along the condensate momentum, \mathbf{k}_0 , consistent with symmetry-expected smectic form, given by (35). The black-dashed contour indicates the degenerate minimum of the noninteracting band $\epsilon_{\mathbf{k}}^-$.

Such nonzero dispersion, with a closed minimum contour is approximately circular for $t_2/t_1 \approx 1/6 + \epsilon$ and can be faithfully modeled by a continuum field theory, encoded in a noninteracting Hamiltonian $H_0 = \int_{\mathbf{r}} \hat{\Psi}_{\mathbf{r}}^\dagger \hat{\epsilon}_{\mathbf{r}} \hat{\Psi}_{\mathbf{r}}$ with,

$$\hat{\epsilon}_{\mathbf{r}} = J(-\nabla^2 - k_0^2)^2 + \epsilon_0, \quad (31)$$

with a quartic dispersion

$$\epsilon_{\mathbf{k}} = J(\mathbf{k}^2 - k_0^2)^2 + \epsilon_0, \quad (32)$$

and minima lying on contour $\mathbf{k}^2 = k_0^2$. The corresponding Euclidean (imaginary-time τ) Lagrangian is given by,

$$\mathcal{L} = \Psi^* \partial_{\tau} \Psi + J |\nabla^2 \Psi|^2 - 2Jk_0^2 |\nabla \Psi|^2 + (\tilde{\epsilon}_0 - \mu) |\Psi|^2 + \frac{U}{2} |\Psi|^4. \quad (33)$$

For $\mu > \epsilon_0$ bosons condense into a nonzero-momentum superfluid state, a simplest version of which is a helical condensate at a single point \mathbf{k}_0 on the dispersion contour minimum – encoded in $\epsilon_{\mathbf{k}}$, (32). In the density-phase representation, the state is characterized by

$$\Psi(\mathbf{r}) = \sqrt{n}e^{i\mathbf{k}_0 \cdot \mathbf{r} + i\phi} = \sqrt{n_0 + \pi}e^{i\mathbf{k}_0 \cdot \mathbf{r} + i\phi} \quad (34)$$

with a nonzero condensate density (at mean-field level) $n_0 = (\mu - \epsilon_0)/U$ and momentum k_0 , for $\mu > \epsilon_0$ (vanishing otherwise), and density and phase fluctuations, π and ϕ , respectively. To quadratic order, the helical superfluid is then described by a Goldstone-mode Lagrangian density, which, after integrating out density field π gives a zero-temperature quantum “columnar” Lagrangian – $m = d - 2$ -Lifshitz model in d space-time dimensions[9] – (to also appear in subsequent sections)

$$\mathcal{L}_\phi \approx B_\tau(\partial_\tau\phi)^2 + B(\partial_\parallel\phi)^2 + K(\partial_\perp^2\phi)^2. \quad (35)$$

At nonzero T , (35) reduces to the classical smectic ($m = d - 1$ -Lifshitz model[9]) Hamiltonian for ϕ discussed in previous subsections.

5. Smectic as a Fulde-Ferrell-Larkin-Ovchinnikov superconductor

A singlet superconductor, frustrated by a depairing Zeeman field has been predicted by Fulde and Ferrell[23] and by Larkin and Ovchinnikov[24] (FFLO) to pair at a nonzero momentum, thereby exhibiting a periodic modulation of the Cooper-pair amplitude – a pair-density wave (PDW)[25, 27]. Such FFLO state, in the absence of deleterious orbital field and pinning lattice effects was proposed[26, 52, 53] to be realizable in spin imbalanced (polarized) Feshbach-resonant paired atomic superfluids. It is now believed to have been observed in an array of decoupled one-dimensional traps, with recent progress toward a higher dimensional realization of the FFLO superfluid.[54]

While microscopic analysis is a bit involved[25, 52, 53], its upshot is a derivation of an effective Landau theory of the form (33) for the pairing amplitude, with a harmonic dispersion ϵ_k , for intermediate Zeeman field (chemical potential for spin imbalance) $h_{c1} < h < h_{c2}$, displaying a minimum on nonzero momentum closed contour, akin to that of the helical superfluid (33), above. Fulde-Ferrell and Larkin-Ovchinnikov are two simplest states that minimize this Lagrangian. The FF state is characterized by a pairing amplitude, [23]

$$\Psi_{FF}(\mathbf{r}) = \Psi_{q_0}e^{i\mathbf{q}_0 \cdot \mathbf{r} + i\phi}, \quad (36)$$

that is a plane-wave with the momentum \mathbf{q}_0 and a single Goldstone mode ϕ , a local superconducting phase. The state carries a nonzero, uniform spontaneously-directed supercurrent

$$\mathbf{j}_{FF} = \frac{1}{m}|\Psi_{q_0}|^2(\mathbf{q}_0 + \nabla\phi), \quad (37)$$

and thereby breaks time-reversal and rotational symmetries, chosen spontaneously along \mathbf{q}_0 , as well as the global gauge symmetry, corresponding to the total atom conservation. The low-energy Lagrangian for $\phi(\mathbf{r}, \tau)$ takes the smectic (columnar at $T = 0$) form, (35).

The LO state[24] is a time-reversal symmetric counterpart, that is a superposition of $\pm\mathbf{q}_0$ paired condensates, given by,

$$\Psi_{LO}(\mathbf{r}) = \Psi_+(\mathbf{r})e^{i\mathbf{q} \cdot \mathbf{r}} + \Psi_-(\mathbf{r})e^{-i\mathbf{q} \cdot \mathbf{r}}, \quad (38a)$$

$$= 2|\Psi_{q_0}|e^{i\frac{1}{2}(\phi_+ + \phi_-)} \cos[\mathbf{q}_0 \cdot \mathbf{r} + \frac{1}{2}(\phi_+ - \phi_-)], \quad (38b)$$

$$= 2|\Psi_{q_0}|e^{i\phi} \cos[\mathbf{q}_0 \cdot \mathbf{r} + \theta]. \quad (38c)$$

It is characterized by the superfluid phase ϕ and the phonon $u = \theta/q_0$ Goldstone modes, with a combination of the XY and smectic sectors in a classical Hamiltonian,

$$\mathcal{H}_{LO} = \frac{1}{2}K(\nabla^2u)^2 + \frac{1}{2}B(\partial_\parallel u - \frac{1}{2}(\nabla u)^2)^2 + \frac{1}{2}\rho_s^\parallel(\partial_\parallel\phi)^2 + \frac{1}{2}\rho_s^\perp(\nabla_\perp\phi)^2, \quad (39)$$

whose zero-temperature quantum counterpart is a combination of XY and “columnar” – $m = d - 2$ -Lifshitz model in d space-time dimensions[9] forms. At nonzero temperature one thus expects FF and LO states to display critical smectic phenomenology that I discuss in the next section.

6. Smectic as quantum Hall stripes

One other prominent example of a quantum smectic has been argued theoretically[18–21] to be realized in half-filled large N Landau level regime and observed experimentally[16, 17] at such filling $\nu = N + 1/2$ through appearance of a highly anisotropic transport below 100 milli-Kelvin. At mean-field level the state is described as a periodic array of alternative integer filling N and $N + 1$ quantum Hall stripes, predicted to be the exact ground state in the $N \gg 1$ limit. Beyond Hartree-Fock theory[18, 19], fluctuations of such a striped state are well described by chiral edge Luttinger liquids, corresponding to inter- (positions) and intra- (shape) stripe phonons of this quantum Hall smectic. Much of the analysis discussed below, importantly beyond its harmonic fluctuations, will also apply to this state at nonzero temperature leading to a critical smectic state. At zero temperature, it is described by “cholesteric”-like, i.e., $m = d - 2$ -Lifshitz model in d space-time dimensions[9].

C. Nonzero T Gaussian fluctuation in a harmonic smectic

To assess the extent of thermal fluctuations of the smectic Goldstone mode $u(\mathbf{r})$ I first analyze them within a harmonic approximation, neglecting elastic nonlinearities in H_{sm} . [4, 55] In terms of the Fourier modes $u_{\mathbf{k}}$, the Hamiltonian decouples, reducing to

$$H_{sm} = \frac{1}{2} \int \frac{d^d k}{(2\pi)^d} (Kk_{\perp}^4 + Bk_z^2) |u_{\mathbf{k}}|^2, \quad (40)$$

thus allowing a straightforward computation of phonon correlation functions via standard Gaussian integrals or equivalently via equipartition. This gives mean-squared fluctuations

$$\langle u^2 \rangle_0^T = \int_{L_{\perp}^{-1}}^{\Lambda_{\perp}} \frac{d^d k}{(2\pi)^d} \frac{T}{Bk_z^2 + Kk_{\perp}^4} \approx \begin{cases} \frac{T}{2\sqrt{BK}} C_{d-1} L_{\perp}^{3-d}, & d < 3, \\ \frac{T}{4\pi\sqrt{BK}} \ln q_0 L_{\perp}, & d = 3, \end{cases} \quad (41)$$

where I defined a constant $C_d = S_d/(2\pi)^d = 2\pi^{d/2}/[(2\pi)^d \Gamma(d/2)]$, with S_d a surface area of a d -dimensional sphere, and introduced an infrared cutoff by considering a system of finite extent $L_{\perp} \times L_z$, with L_z the length of the system along the ordering (z) axis and L_{\perp} transverse to z . Unless it has a huge aspect ratio, such that $L_z \sim L_{\perp}^2/\lambda \gg L_{\perp}$, any large system ($L_{\perp}, L_z \gg \lambda$) will have $\lambda L_z \ll L_{\perp}^2$.

The key observation here is that the smectic phonons exhibit fluctuations that diverge, growing logarithmically in 3d and linearly in 2d with system size L_{\perp} ; for $d > 3$ fluctuations are bounded. Thus, as a consequence of their “soft” elasticity (a vanishing $(\nabla_{\perp} u)^2$ modulus) 3d smectics are akin to 2d XY systems, such as superfluid films and two-dimensional crystals, [8, 56–59], exhibit a power-law order in three dimensions.

The expression for the mean-squared phonon fluctuations in (41) leads the emergence of important crossover length scales ξ_{\perp}, ξ_z , related by

$$\xi_{\perp} = (\xi_z \sqrt{K/B})^{1/2} \equiv \sqrt{\xi_z \lambda}, \quad (42)$$

that characterize the finite-temperature smectic state. These are defined as scales L_{\perp}, L_z at which phonon fluctuations are large, comparable to the smectic period $a = 2\pi/q_0$. Namely, setting

$$\langle u^2 \rangle_0^T \approx a^2 \quad (43)$$

in Eq. (41) one finds

$$\xi_{\perp} \approx \begin{cases} \frac{a^2 \sqrt{BK}}{T} \sim \frac{K}{Tq_0}, & d = 2, \\ ae^{4\pi a^2 \sqrt{BK}/T} \sim ae^{\frac{cK}{Tq_0}}, & d = 3, \end{cases} \quad (44)$$

where in the second form of the above expressions I took the simplest approximation for the smectic anisotropy length $\lambda = \sqrt{K/B}$ to be $\lambda = a \sim 1/q_0$, and introduced $O(1)$ Lindemann constant c , [60] that depends on the somewhat arbitrary definition of “large” phonon root-mean-squared fluctuations.

The smectic connected correlation function

$$C_u(\mathbf{x}_{\perp}, z) = \langle [u(\mathbf{x}_{\perp}, z) - u(\mathbf{0}, 0)]^2 \rangle_0. \quad (45)$$

is also straightforwardly worked out, in 3d giving the logarithmic Caillé form[55]

$$C_u^{3d}(\mathbf{x}_\perp, z) = 2T \int \frac{d^2k_\perp dk_z}{(2\pi)^3} \frac{1 - e^{i\mathbf{k}\cdot\mathbf{x}}}{Kk_\perp^4 + Bk_z^2} \equiv \frac{T}{2\pi\sqrt{KB}} g_T^{3d} \left(\frac{z\lambda}{x_\perp^2}, \frac{x_\perp}{a} \right) \quad (46a)$$

$$= \frac{T}{2\pi\sqrt{KB}} \left[\ln \left(\frac{x_\perp}{a} \right) - \frac{1}{2} \text{Ei} \left(\frac{-x_\perp^2}{4\lambda|z|} \right) \right], \quad (46b)$$

$$\approx \frac{T}{2\pi\sqrt{KB}} \begin{cases} \ln \left(\frac{x_\perp}{a} \right), & x_\perp \gg \sqrt{\lambda|z|}, \\ \ln \left(\frac{4\lambda z}{a^2} \right), & x_\perp \ll \sqrt{\lambda|z|}, \end{cases} \quad (46c)$$

where $\text{Ei}(x)$ is the exponential-integral function. As indicated in the last form, in the asymptotic limits of $x_\perp \gg \sqrt{\lambda z}$ and $x_\perp \ll \sqrt{\lambda z}$ above 3d correlation function reduces to a logarithmic growth with x_\perp and z , respectively.

In 2d one instead finds[61]

$$C_u^{2d}(x, z) = 2T \int \frac{dk_x dk_z}{(2\pi)^2} \frac{1 - e^{i\mathbf{k}\cdot\mathbf{x}}}{Kk_x^4 + Bk_z^2} \equiv \frac{T}{2\pi\sqrt{KB}} g_T^{2d} \left(\frac{z\lambda}{x^2}, \frac{x}{a} \right), \quad (47a)$$

$$= \frac{2T}{B} \left[\left(\frac{|z|}{4\pi\lambda} \right)^{1/2} e^{-x^2/(4\lambda|z|)} + \frac{|x|}{4\lambda} \text{erf} \left(\frac{|x|}{\sqrt{4\lambda|z|}} \right) \right] \quad (47b)$$

$$\approx \frac{2T}{B} \begin{cases} \left(\frac{|z|}{4\pi\lambda} \right)^{1/2}, & x \ll \sqrt{\lambda|z|}, \\ \frac{|x|}{4\lambda}, & x \gg \sqrt{\lambda|z|}, \end{cases} \quad (47c)$$

where $\text{erf}(x)$ is the Error function.

As a consequence of above divergent phonon fluctuations, the smectic density wave order parameter (11) vanishes in thermodynamic limit

$$\langle \rho(\mathbf{x}) \rangle_0 = 2|\rho_q| \langle \cos[\mathbf{q}_0 \cdot \mathbf{x} - qu(\mathbf{x})] \rangle_0, \quad (48a)$$

$$= 2|\rho_q| e^{-\frac{1}{2}q_0^2 \langle u^2 \rangle_0} \cos(\mathbf{q}_0 \cdot \mathbf{x}), \quad (48b)$$

$$= 2\tilde{\rho}_q(L_\perp) \cos(\mathbf{q}_0 \cdot \mathbf{x}), \quad (48c)$$

with the thermally suppressed order parameter amplitude given by

$$\tilde{\rho}_q(L_\perp) = |\rho_q| \begin{cases} e^{-L_\perp/\xi_\perp}, & d = 2, \\ \left(\frac{a}{L_\perp} \right)^{\eta/2}, & d = 3, \end{cases} \quad (49a)$$

$$\rightarrow 0, \quad \text{for } L_\perp \rightarrow \infty, \quad (49b)$$

where I used results for the phonon and phase fluctuations, (41), and defined the Caillé exponent

$$\eta = \frac{q_0^2 T}{8\pi\sqrt{BK}}. \quad (50)$$

Thus, in qualitative contrast to its mean-field cartoon, at long scales (longer than $\xi_{\perp,z}$) the smectic state is actually characterized by a *uniform* mass density.

Since the average density is actually uniform, a better characterization of the smectic state is through the structure function, $S(\mathbf{q})$, a Fourier transform of the density correlation function, that in 3d is given by

$$S(\mathbf{q}) = \int d^3x \langle \delta\rho(\mathbf{x}) \delta\rho(0) \rangle e^{-i\mathbf{q}\cdot\mathbf{x}}, \quad (51a)$$

$$\approx \frac{1}{2} \sum_{q_n} |\rho_{q_n}|^2 \int_{\mathbf{x}} \langle e^{-iq_n(u(\mathbf{x})-u(0))} \rangle_0 e^{-i(\mathbf{q}-q_n\hat{z})\cdot\mathbf{x}}, \quad (51b)$$

$$\approx \frac{1}{2} \sum_n \frac{|\rho_{q_n}|^2}{|q_z - nq_0|^{2-n^2\eta}}, \quad \text{for } d = 3, \quad (51c)$$

where I approximated phase and phonon fluctuations by Gaussian statistics (in 3d valid up to weak logarithmic corrections[11]). Thus as anticipated one finds that the logarithmically divergent 3d phonon fluctuations lead to a

structure function, with highly anisotropic ($q_z \sim q_\perp^2/\lambda$) *quasi*-Bragg peaks replacing the true (δ -function) Bragg peaks characteristic of a true long-range periodic order.[4, 10, 62]

In two dimensions, smectic order is even more strongly suppressed by thermal fluctuations. The linear growth of the 2d phonon fluctuations leads to exponentially short-ranged correlations of the density, expected to result in dislocation unbinding at any nonzero temperature, thereby completely destroying smectic state in 2d.[61]

D. Nonlinear elasticity: beyond Gaussian fluctuations

1. Perturbation theory

As is clear from the analysis of the previous subsection, the restoration of the translational symmetry (a vanishing $\langle \rho_q(\mathbf{x}) \rangle$, etc.) by thermal fluctuations is a robust prediction of the quadratic theory, that cannot be overturned by the left-out nonlinearities. However, as discussed in the Introduction and illustrated instability of the smectic Gaussian fixed point (in $d < 3$) in Fig.3, the asymptotic long-scale form of the correlation functions computed within the harmonic approximation only extends out to the nonlinear length scales $\xi_{\perp,z}^{NL}$. On longer scales, the divergently large smectic phonon fluctuations invalidate the neglect of phonon nonlinearities,

$$\mathcal{H}_{\text{nonlinear}} = -\frac{1}{2}B(\partial_z u)(\nabla u)^2 + \frac{1}{8}B(\nabla u)^4. \quad (52)$$

These will necessarily qualitatively modify predictions (46c), (47c), and (51) on scales longer than the crossover scales $\xi_{\perp,z}^{NL}$, that I compute next.

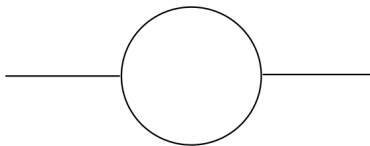


FIG. 6: Feynman graph that renormalizes the elastic moduli K , B of the smectic state.

To see this, one uses a perturbative expansion in the nonlinear operators (52) to assess the size of their contribution to e.g., the free energy. Following the standard field-theoretic RG analysis, pioneered by Wilson and Fisher[1] (but here applied to the critical smectic phase, rather than to a critical point) these can be accounted for as corrections to the compressional B and bend K elastic moduli, with the leading softening (negative) contribution to δB , summarized graphically in Fig.6, and given by

$$\delta B = -\frac{1}{2}TB^2 \int_{\mathbf{q}} q_\perp^4 G_u(\mathbf{q})^2, \quad (53a)$$

$$\begin{aligned} &\approx -\frac{1}{2}TB^2 \int_{-\infty}^{\infty} \frac{dq_z}{2\pi} \int_{L_\perp^{-1}} \frac{d^{d-1}q_\perp}{(2\pi)^{d-1}} \frac{q_\perp^4}{(Kq_\perp^4 + Bq_z^2)^2}, \\ &\approx -\frac{1}{8} \frac{C_{d-1}T}{3-d} \left(\frac{B}{K^3} \right)^{1/2} L_\perp^{3-d} B. \end{aligned} \quad (53b)$$

In above, I used the smectic correlator, $G_u(\mathbf{q})$, focused on $d \leq 3$ (which allowed the dropping of the uv-cutoff (Λ) dependent part that vanishes for $\Lambda \rightarrow \infty$), and cutoff the divergent contribution of the long wavelength modes via the infra-red cutoff $q_\perp > 1/L_\perp$ by considering a system of a finite extent L_\perp . Similar analysis gives a *positive* fluctuation correction to the bend modulus K , stiffening the undulation mode.[25]

Clearly the anharmonicity becomes important when the fluctuation corrections to the elastic constants (e.g., δB above) become comparable to its bare microscopic value. As the analysis below demonstrates, the divergence of this correction as $L_\perp \rightarrow \infty$ signals the breakdown of the conventional harmonic elastic theory on length scales longer than a crossover scale

$$\xi_\perp^{NL} \approx \begin{cases} \frac{1}{T} \left(\frac{K^3}{B} \right)^{1/2}, & d = 2, \\ ae^{\frac{c}{T}} \left(\frac{K^3}{B} \right)^{1/2}, & d = 3, \end{cases} \quad (54)$$

which I define here as the value of L_{\perp} at which $|\delta B(\xi_{\perp}^{NL})| = B$. Within the approximation of the smectic screening length $\lambda = a$, these nonlinear crossover lengths reduce to the phonon disordering lengths (42), (44), defined by the Lindemann-like criterion.[60] Clearly, on scales longer than $\xi_{\perp,z}^{NL}$ (also a crossover scale from Gaussian to smectic fixed point in Fig.1) the perturbative contributions of nonlinearities dominate and therefore cannot be neglected. Their contribution are thus expected to qualitatively modify the harmonic predictions of the previous subsection.

2. Renormalization group analysis in $d = 3 - \epsilon$ dimensions

To describe the physics beyond the crossover scales, $\xi_{\perp,z}^{NL}$ – i.e., to make sense of the infra-red divergent perturbation theory found in Eq.53b – requires a renormalization group analysis.[1–3] This was first performed in the context of conventional 3d smectic liquid crystals and Lifshitz points in a seminal work by Grinstein and Pelcovits (GP)[11]. Below, I complement GP’s treatment with Wilson’s momentum-shell renormalization group (RG) analysis, extending it to an arbitrary dimension d , so as to connect to the behavior in 2d, that has an exact solution[63].

To this end I integrate (perturbatively in $\mathcal{H}_{\text{nonlinear}}$) short-scale Goldstone modes in an infinitesimal cylindrical shell of wavevectors, $\Lambda e^{-\delta\ell} < q_{\perp} < \Lambda$ and $-\infty < q_z < \infty$ ($\delta\ell \ll 1$ is infinitesimal). The leading perturbative momentum-shell coarse-graining contributions come from terms found in direct perturbation theory above, but with the system size divergences controlled by the infinitesimal momentum shell. The thermodynamic averages can then be equivalently carried out with an effective coarse-grained Hamiltonian of the form (8), with momentum-dependent couplings obtained from integrating up their infinitesimal corrections, obtained via momentum-shell RG. For smectic moduli B and K this gives,

$$\delta B \approx -\frac{1}{8}gB\delta\ell, \quad \delta K \approx \frac{1}{16}gK\delta\ell, \quad (55)$$

where the dimensionless coupling is given by

$$g = C_{d-1}\Lambda_{\perp}^{d-3}T \left(\frac{B}{K^3}\right)^{1/2} \approx \frac{T}{2\pi} \left(\frac{B}{K^3}\right)^{1/2}, \quad (56)$$

and in the second form I approximated g by its value in 3d. Eqs.(55) show that B is softened and K is stiffened by the nonlinearities in the presence of thermal fluctuations, making the system effectively more isotropic, as one may expect on general physical grounds.

For convenience I then anisotropically rescale the lengths and the remaining long wavelength part of the fields $u^<(\mathbf{r})$ according to $r_{\perp} = r'_{\perp} e^{\delta\ell}$, $z = z' e^{\omega\delta\ell}$ and $u^<(\mathbf{r}) = e^{\phi\delta\ell} u'(\mathbf{r}')$, so as to restore the ultraviolet cutoff $\Lambda_{\perp} e^{-\delta\ell}$ back up to Λ_{\perp} . The underlying rotational invariance ensures that the nonlinear fluctuation corrections preserve the rotationally invariant strain operator $(\partial_z u - \frac{1}{2}(\nabla_{\perp} u)^2)$, renormalizing it as a whole. It is therefore convenient (but not necessary) to choose the dimensional rescaling that also preserves this form. It is easy to see that this choice leads to

$$\phi = 2 - \omega. \quad (57)$$

The leading (one-loop) corrections to the effective coarse-grained and rescaled free energy functional can then be summarized by differential RG flows

$$\frac{dB(\ell)}{d\ell} = (d + 3 - 3\omega - \frac{1}{8}g(\ell))B(\ell), \quad (58a)$$

$$\frac{dK(\ell)}{d\ell} = (d - 1 - \omega + \frac{1}{16}g(\ell))K(\ell). \quad (58b)$$

From these one readily obtains the flow of the dimensionless coupling $g(\ell)$

$$\frac{dg(\ell)}{d\ell} = (3 - d)g - \frac{5}{32}g^2, \quad (59)$$

whose flow for $d < 3$ away from the $g = 0$ Gaussian fixed point encodes the long-scale divergences found in the direct perturbation theory above. This resembles the Wilson-Fisher flow at the critical point just below $d = 4$ [1], but, as discussed in the Introduction requires no fine tuning. As summarized in Fig.3 for $d < 3$ the flow terminates at a nonzero fixed-point coupling $g_* = \frac{32}{5}\epsilon$ (with $\epsilon \equiv 3 - d$), that determines the nontrivial long-scale behavior of the smectic critical phase (see below). As with treatments of critical points[1, 4], but here extending over the whole

smectic phase, the RG procedure is quantitatively justified by the proximity to $d = 3$, i.e., controlled by the smallness of ϵ .

One can now use a standard matching calculation to determine the long-scale asymptotic form of the correlation functions on scales beyond $\xi_{\perp,z}^{NL}$. Namely, applying above coarse-graining RG analysis to a computation of correlation functions allows one to relate its form at long length scales of interest (that, because of infrared divergences is impossible to compute via a direct perturbation theory in nonlinearities) to its counterpart at short scales, evaluated with coarse-grained couplings, $B(\ell)$, $K(\ell)$, \dots . In contrast to the former, the latter is readily computed via a perturbation theory, that, because of shortness of the length scale is convergent. The result of this matching calculation to lowest order gives correlation functions from an effective Gaussian theory,

$$G_u(\mathbf{k}) \approx \frac{T}{B(\mathbf{k})k_z^2 + K(\mathbf{k})k_{\perp}^4}, \quad (60)$$

with moduli $B(\mathbf{k})$ and $K(\mathbf{k})$ that are singularly wavevector-dependent, determined by the solutions $B(\ell)$ and $K(\ell)$ of the RG flow equations (58a) and (58b), with initial conditions given by the microscopic values B and K .

2d analysis: In $d = 2$, at long scales $g(\ell)$ flows to a nontrivial infrared stable fixed point $g_* = 32/5$, and the matching analysis predicts correlation functions characterized by anisotropic wavevector-dependent moduli

$$K(\mathbf{k}) = K(k_{\perp}\xi_{\perp}^{NL})^{-\eta_K} f_K(k_z\xi_z^{NL}/(k_{\perp}\xi_{\perp}^{NL})^{\zeta}), \quad (61a)$$

$$\sim k_{\perp}^{-\eta_K},$$

$$B(\mathbf{k}) = B(k_{\perp}\xi_{\perp}^{NL})^{\eta_B} f_B(k_z\xi_z^{NL}/(k_{\perp}\xi_{\perp}^{NL})^{\zeta}), \quad (61b)$$

$$\sim k_{\perp}^{\eta_B}.$$

Thus, on scales longer than $\xi_{\perp,z}^{NL}$ these qualitatively modify the real-space correlation function asymptotics of the harmonic analysis in the previous subsection. In Eqs.(61) the universal anomalous exponents are given by

$$\eta_B = \frac{1}{8}g_* = \frac{4}{5}\epsilon, \quad (62a)$$

$$\approx \frac{4}{5}, \quad \text{for } d = 2,$$

$$\eta_K = \frac{1}{16}g_* = \frac{2}{5}\epsilon, \quad (62b)$$

$$\approx \frac{2}{5}, \quad \text{for } d = 2,$$

determining the $z - \mathbf{x}_{\perp}$ anisotropy exponent via (60) to be

$$\zeta \equiv 2 - (\eta_B + \eta_K)/2, \quad (63a)$$

$$= \frac{7}{5}, \quad \text{for } d = 2, \quad (63b)$$

as expected reduced by thermal fluctuations down from its harmonic value of 2. The $\mathbf{k}_{\perp} - k_z$ dependence of $B(\mathbf{k})$, $K(\mathbf{k})$ is determined by universal scaling functions, $f_B(x)$, $f_K(x)$ that I will not compute here. The underlying rotational invariance gives an *exact* relation between the two anomalous $\eta_{B,K}$ exponents

$$3 - d = \frac{\eta_B}{2} + \frac{3}{2}\eta_K, \quad (64a)$$

$$1 = \frac{\eta_B}{2} + \frac{3}{2}\eta_K, \quad \text{for } d = 2, \quad (64b)$$

which is obviously satisfied by the anomalous exponents, Eqs.(62b),(62a), computed here to first order in $\epsilon = 3 - d$.

Thus, as advertised, I find that at nonzero temperature, a 2d smectic state is highly nontrivial and qualitatively distinct from its mean-field perfectly periodic form. In addition to a vanishing density modulation and associated fluctuation-restored translational symmetry, it is characterized by universal nonlocal length-scale dependent moduli, Eq. (61). Consequently its Goldstone mode theory and the associated correlations are not describable by a local harmonic field theory, that is an analytic expansion in local field operators. Instead, in 2d, on length scales beyond $\xi_{\perp,z}^{NL}$ (but shorter than the expected dislocation unbinding length ξ_{disl}) thermal fluctuations and correlations of this smectic *critical* phase are controlled by a nontrivial fixed point, illustrated in Fig. 3, characterized by *universal* anomalous exponents $\eta_{K,B}$ and scaling functions $f_{B,K}(x)$, defined above.

Above I obtained this nontrivial structure from an RG analysis and estimated these exponents within a controlled but approximate ϵ -expansion. Remarkably, in 2d an exact solution of this problem was discovered by Golubovic and Wang[63]. It predicts critical phenomenology in a qualitatively agreement with the RG predictions above, and gives exact exponents

$$\eta_B^{2d} = 1/2, \quad \eta_K^{2d} = 1/2, \quad \zeta^{2d} = 3/2, \quad (65)$$

derived by mapping onto the 1+1d KPZ equation.[64]

3d analysis: In $d = 3$, the nonlinear coupling $g(\ell)$ is marginally irrelevant, flowing to 0 at long scales. Despite this, as discovered by Larkin and Khmel'nitskii and by Michael Fisher, et al., in the context of the Ising model[2, 65, 66], the marginal flow to the Gaussian fixed point is sufficiently slow (logarithmic in lengths) that (as usual at a marginal dimension[4]) its power-law in ℓ dependence leads to a universal, asymptotically *exact* logarithmic wavevector dependence found in a smectic by Grinstein and Pelcovits[11],

$$K(\mathbf{k}_\perp, k_z = 0) \sim K \left| 1 + \frac{5g}{64\pi} \ln(1/k_\perp a) \right|^{2/5}, \quad (66a)$$

$$B(\mathbf{k}_\perp = 0, k_z) \sim B \left| 1 + \frac{5g}{128\pi} \ln(\lambda/k_z a^2) \right|^{-4/5}. \quad (66b)$$

This translates into the smectic order parameter correlations given by

$$\langle \rho_q^*(\mathbf{x}) \rho_q(0) \rangle \sim e^{-c_1 (\ln z)^{6/5}} \cos(q_0 z), \quad (67)$$

with $2/5, 4/5$, and $6/5$ *exact* universal exponents and c_1 a nonuniversal constant[11]. Although these 3d anomalous effects are less dramatic and likely to be difficult to observe in practice, theoretically they are quite significant as they represent a qualitative breakdown of the mean-field and harmonic descriptions, that respectively ignore interactions and thermal fluctuations.

I conclude this section by noting that all of the above analysis is predicated the validity of the purely elastic model, Eq. (8), that neglects topological defects, such as dislocations. If these unbind (as they undoubtedly do in 2d at any nonzero temperature[61]), then above prediction only hold on scales shorter than the separation ξ_{disl} between these defects.

III. BIAXIALLY PERIODIC CRITICAL STATES: SPONTANEOUS LINE-CRYSTALS

Another class of critical states are those partially crystalized along *two* of the three axes. They can be dubbed as “*spontaneous* line-crystals” as they are a periodic 2d crystalline array of 1d liquids, oriented along a *spontaneously* chosen axis, illustrated in Fig.2(c), and in this sense dual to a uniaxially periodic critical state – a 1d periodic array of 2d liquids – the $m = d - 1$ -Lifshitz model[9], discussed in Sec.II. As I discuss below, its key feature is rotational symmetry-enforced vanishing of the tilt modulus – the $m = 1$ -Lifshitz model[9], that leads to its enhanced critical fluctuations.

A. Columnar liquid crystal

One example of a spontaneous line-crystal is a ubiquitous “columnar” liquid crystal. It emerges from a nematic fluid composed of a high aspect ratio disk-shaped constituents, illustrated in Fig. 2(c).[10] In this phase disk-shaped molecules stack into one-dimensional fluid columns along a spontaneous nematic axis, that freeze into a 2d crystal (typically triangular lattice), retaining fluid order along the columns. Such discotic liquid crystal, forming a 2d crystal of 1d fluid columns compliments the smectic state of 1d periodic array of 2d fluids, discussed in earlier sections.

Simple analysis similar to that of a smectic, shows that for $d < 5/2$ the columnar liquid crystal ($m = 1$ -Lifshitz model[9]) is a critical phase, though given this dimensional constraint not a very practical one for experimental realization. However, although I do not pursue the subject here, I note that far stronger distortion effects of quenched disorder (e.g., columnar state in aerogel[12–14]) lead to a critical columnar glass for $d < 7/2$, characterized by an infrared attractive fixed point controlled by disorder.[39]

The columnar state is characterized by a two-component phonon field $\mathbf{u} = (u_x, u_y)$, that are two Goldstone modes associated with translational symmetry breaking in the plane transverse to the columns. Analogously to a smectic, the Goldstone modes associated with the rotational symmetry are gapped out by the emergent Higgs mechanism.[32]

Although one can derive the Goldstone mode elasticity for the columnar state by following the approach analogous to that of a smectic, here I will simply write it down based on symmetry and experience with the smectic. To this

end I note that the columnar state exhibits two types of rigidities, the in-plane (transverse to the columnar axis \hat{z}) crystalline elasticity and bending elasticity of the columns. The former is characterized by shear and bulk elasticity of a 2d crystal. The latter is captured by the higher-derivative curvature (rather than tension) filament elasticity. Together these give the energy density

$$\mathcal{H}_{col} = \frac{1}{2}\kappa(\partial_z^2 \mathbf{u})^2 + \frac{\lambda}{2} u_{\alpha\alpha}^2 + \mu u_{\alpha\beta}^2, \quad (68)$$

where κ is the curvature modulus, μ and λ are Lamé elastic moduli of 2d triangular lattice[4], and (with the summation convention over repeated indices) the strain tensor is given by

$$u_{\alpha\beta} = \frac{1}{2} \left(\partial_\alpha u_\beta + \partial_\beta u_\alpha - \partial_\gamma u_\alpha \partial_\gamma u_\beta \right) \approx \frac{1}{2} \left(\partial_\alpha u_\beta + \partial_\beta u_\alpha - \partial_z u_\alpha \partial_z u_\beta \right). \quad (69)$$

The two phonons, $\mathbf{u}(x, y, z) = (u_x, u_y)$ are fields in a three-dimensional space, and in the second approximate form above I only kept the most important strain nonlinearities.

As in the discussion of the smectic elasticity, the columnar nonlinear elasticity (68) is strictly constrained by symmetry. The linear z derivative in the harmonic terms is forbidden by the rotational invariance about the x axes (broken spontaneously), at infinitesimal level corresponding to $\mathbf{u} \rightarrow \mathbf{u} + \theta z \hat{\mathbf{y}}$. This “softness” with respect to $\partial_z \mathbf{u}$ modes then requires one to keep corresponding nonlinearities in the in-plane strain tensor, $u_{\alpha\beta}$ above, the form of which is dictated by the in-plane rotational invariance.

As in a smectic, here too the analysis of quadratic phonon fluctuations leads to power-law divergence for $d < 5/2$, requiring inclusion of elastic nonlinearities in (68) via (69). Account of these via an RG analysis very similar to that of the smectic in the previous section, leads to a nontrivial infrared stable fixed point controlled by $\epsilon = 5/2 - d$, that characterizes the universal properties of the resulting columnar *critical phase* (as in Fig.3). For technical details, I refer the reader to the original literature.[39]

B. Spontaneous vortex lattice in magnetic superconductors

Another putative realization of a biaxially periodic (line-crystal) critical state is a “spontaneous vortex lattice” in a ferromagnetic superconductor (FS). Rare-earth borocarbide materials are believed to be examples of the latter, exhibiting a rich phase diagram that includes superconductivity, antiferromagnetism, ferromagnetism and spiral magnetic order.[36–38] In particular, there is now ample experimental evidence that, at low temperatures, superconductivity and ferromagnetism competitively coexist in $\text{ErNi}_2\text{B}_2\text{C}$ compounds, and perhaps in more recently discovered high temperature superconductor $\text{Sr}_2\text{Y Ru}_{1-x}\text{Cu}_x\text{O}_6$.

For sufficiently strong ferromagnetism, such FS’s have been predicted[38] to exhibit a *spontaneous* vortex (SV) state driven by the spontaneous magnetization, rather than by an external magnetic field \mathbf{H} . It is clear based purely on symmetry arguments that for $\mathbf{H} = 0$ and in the absence of atomic crystal anisotropy, the elastic properties of the resulting SV solid differ dramatically and *qualitatively* from those of a conventional Abrikosov lattice. The key underlying difference is the aforementioned *vanishing* of the tilt modulus (68), which is guaranteed by the underlying rotational invariance. Although this invariance is broken by the magnetization, \mathbf{M} , the tilt modulus remains zero because this breaking is *spontaneous* (neglecting the ever-present crystal field anisotropy). This contrasts strongly with a conventional vortex solid, where the rotational symmetry is *explicitly* broken by the *applied* field \mathbf{H} and lattice anisotropy.

Consequently, the elasticity of the SV crystal is identical to that of the columnar phase, described by(68) together with (69), neglecting crystalline anisotropy. In the presence of purely thermal fluctuations, elastic nonlinearities remain irrelevant for such 3d SV state, since $d = 3 > 5/2$. However, as discovered and explored in Refs. 40, 41, in the presence of ever-present quenched disorder, SV is a disorder- (rather than temperature-) controlled critical glass state, treatable via RG perturbative in $\epsilon = 7/2 - d$, with many interesting properties, e.g., the unusually singular $B(H)$ relation.

IV. POLYMERIZED MEMBRANE

A fluctuating, *tensionless* and therefore curvature-(as opposed to tension-) controlled membrane is a strongly fluctuating system. Focus on such membranes was originally stimulated in part by ubiquitous biophysical realizations (e.g., liposomes, cellular membranes, cytoskeleton of a red blood cell, etc)[44], but more recently found an ideal realization in fluctuating graphene sheets.[67] The latter, polymerized (solid) membrane, characterized by a nonzero in-plane shear rigidity, is particularly fascinating case of a critical phase for its internal dimension $D < 4$.

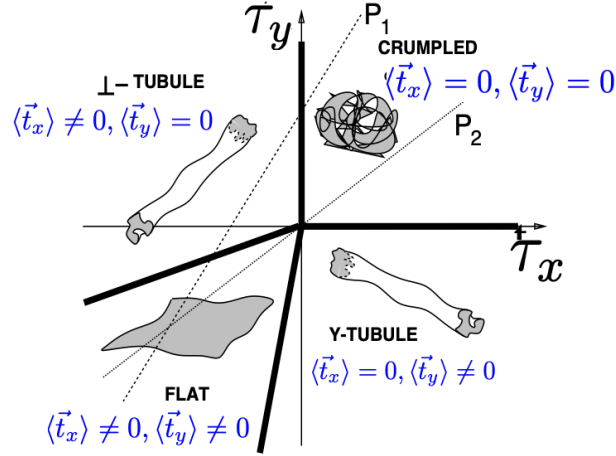


FIG. 7: Illustration of a phase diagram of a polymerized membrane, controlled by temperature and in-plane anisotropy encoded in reduced temperatures τ_x and τ_y . An isotropic membrane is described by $\tau_x = \tau_y \equiv \tau$, exhibiting temperature τ - driven transition along path P_2 from a crumpled phase (with vanishing tangent $\vec{t}_{x,y} = 0$ order parameters) to a “flat” phase a phase with $\vec{t}_{x,y} \neq 0$. Flat phase spontaneously breaks the rotational $O(3)$ symmetry of the embedding space and is a critical phase that exhibits rich universal power-law phenomenology, controlled by a nontrivial infrared stable fixed point. A polymerized membrane with in-plane anisotropy is predicted to undergo a two-stage transition along P_1 from the crumpled-to-tubule phase (latter characterized by only one of the two tangent order parameters nonzero), followed by tubule-to-flat phase transition[68, 69], later observed in simulations.[70]

As was first argued by Nelson and Peliti[45], in addition to the rotationally invariant “crumpled” phase of linear polymers and liquid membranes, polymerized membranes exhibit a finite temperature “flat” phase. As I will discuss below, this too is a *critical* phase characterized by universal power-law correlations (e.g., membrane roughness) and anomalous elasticity, with the state’s very existence in two-dimensional membranes being a beautiful illustration of a phenomena of order-from-disorder. I note in passing that, as illustrated in Fig.7, a non-self-avoiding – “phantom”

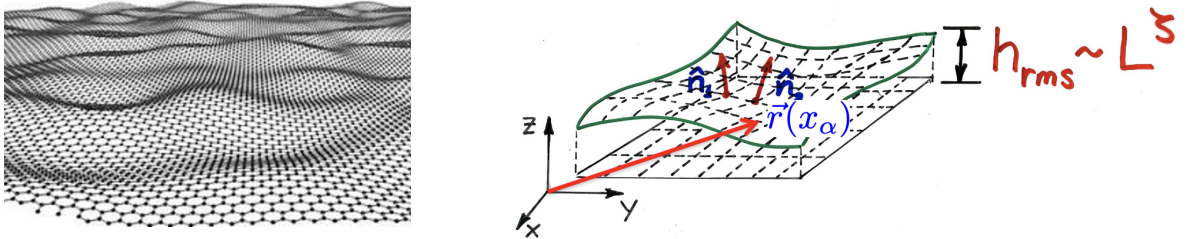


FIG. 8: Illustration of (a) a graphene sheet as a modern ideal realization of a thermally fluctuating polymerized membrane, predicted to exhibit rich anomalous elasticity as a critical phase, (b) flat phase of a polymerized membrane defining its normals, Monge gauge embedding and the definition of the roughness exponent, ζ .

anisotropic polymerized membrane was predicted[68, 69] and observed in simulations[70] to exhibit an intermediate tubule phase, crumpled along one dimension and extended along the other, that, despite its one-dimensionality, is stable to thermal fluctuations.

A detailed derivation of the flat-phase Goldstone-modes elasticity is available[44, 45] starting from the Landau theory of the crumpled phase in terms of the tangent vectors $\nabla \vec{r}(\mathbf{x})$, where $\vec{r}(\mathbf{x})$ is the embedding of the D -dimensional membrane (parameterized by \mathbf{x}) in the d -dimensional space, \vec{r} (with $D = 2$ and $d = 3$ the physical case). The flat phase parameterized by

$$\vec{r}(\mathbf{x}) = (t_0 \mathbf{x} + \mathbf{u}(\mathbf{x}), \vec{h}(\mathbf{x})), \quad (70)$$

in the Monge gauge, spontaneously breaks the $O(d)$ symmetry of the crumpled phase down to $O(D)$, where t_0 scale factor is the effective order parameter of the flat phase, $\mathbf{u}(\mathbf{x})$ is the D -component in-plane phonon, and $\vec{h}(\mathbf{x})$ is

the ‘‘height function’’ describing the membrane’s transverse undulation into the embedding space; we have implicitly generalized to arbitrary co-dimension $d_c = d - D$.

The resulting energy functional is a sum of the bending and the in-plane elastic contributions:

$$H_{flat}[\vec{h}, \mathbf{u}] = \int d^D x \left[\frac{\kappa}{2} (\nabla^2 \vec{h})^2 + \mu u_{\alpha\beta}^2 + \frac{\lambda}{2} u_{\alpha\alpha}^2 \right], \quad (71)$$

where the nonlinear strain tensor is

$$u_{\alpha\beta} = \frac{1}{2} (\partial_\alpha \vec{r} \cdot \partial_\beta \vec{r} - \delta_{\alpha\beta}) \approx \frac{1}{2} (\partial_\alpha u_\beta + \partial_\beta u_\alpha + \partial_\alpha \vec{h} \cdot \partial_\beta \vec{h}), \quad (72)$$

defined as the deviation of the embedding-induced metric $g_{\alpha\beta}$ from the flat metric, and in the second form I neglected elastic nonlinearities that are subdominant at long scales. A crucial feature of $H_{flat}[\vec{h}, \mathbf{u}]$ (71) (as with other critical phases) is the higher-order curvature elasticity of \vec{h} , with the surface tension modulus for $(\nabla \vec{h})^2$ vanishing exactly, enforced by the underlying rotational invariance (of the embedding space) and tension-free membrane.

One can also integrate out the noncritical in-plane phonon field \mathbf{u} , that appears only harmonically, to obtain a convenient equivalent form, purely in terms of \vec{h} [45, 46, 49, 71]

$$H_{flat}[\vec{h}] = \int d^D x \left[\frac{\kappa}{2} (\nabla^2 \vec{h})^2 + \frac{1}{4d_c} (\partial_\alpha \vec{h} \cdot \partial_\beta \vec{h}) R_{\alpha\beta,\gamma\delta} (\partial_\gamma \vec{h} \cdot \partial_\delta \vec{h}) \right] \quad (73)$$

where for convenience, I rescaled Lamé coefficients so that the quartic coupling is of order $1/d_c$. The four-point coupling fourth-rank tensor is given by

$$R_{\alpha\beta,\gamma\delta} = \frac{K - 2\mu}{2(D - 1)} P_{\alpha\beta}^T P_{\gamma\delta}^T + \frac{\mu}{2} (P_{\alpha\gamma}^T P_{\beta\delta}^T + P_{\alpha\delta}^T P_{\beta\gamma}^T), \quad (74)$$

where $P_{\alpha\beta}^T = \delta_{\alpha\beta} - q_\alpha q_\beta / q^2$ is a transverse (to \mathbf{q}) projection operator. The convenience of this decomposition is that $K = 2\mu(2\mu + D\lambda)/(2\mu + \lambda)$ and μ moduli renormalize independently and multiplicatively.[48, 71]

I note that this last h -only elastic form indeed reflects the general discussion of critical phases in the Introduction, namely that they are described by an energy functional (of ϕ^4 form with $\vec{\phi}_\alpha \equiv \partial_\alpha \vec{h}$) enforced to be critical (i.e., missing the ϕ^2 term) by the underlying rotational symmetry, as illustrated in Fig.3.

Applying Wilson-Fisher momentum-shell RG analysis to membrane’s elastic nonlinearities[45–48, 71] one sees that for $D < 4$ (and arbitrary embedding dimension d) the membrane exhibits height undulations that diverge with its extent L . As for smectics and other critical phases discussed earlier, one can make sense of the associated divergent perturbation theory in elastic nonlinearities by performing an RG analysis controlled by $\epsilon = 4 - D$ [46] or equivalently $1/d_c$ (large embedding dimension, that is the analog of $1/N$ large N expansion of the $O(N)$ model’s Wilson-Fisher critical point)[47]. The RG approach for arbitrary d gives flows of the dimensionless nonlinear coupling constants, $\hat{\mu}(\ell) = \mu/\kappa^2, \hat{\lambda}(\ell) = \lambda/\kappa^2$, after integrating out modes in a momentum shell $\Lambda e^{-\delta\ell} < q < \Lambda$ (as for a smectic in previous section), and rescaling for convenience.

The dimensionless couplings flow to a tuning-free infrared attractive Aronovitz-Lubensky (AL) fixed point,[45–48], with two other (in addition to the Gaussian) fixed points that describe a marginally mechanically unstable membrane (of physical relevance to nematic elastomers of the next section). The resulting globally infrared stable AL fixed point controls the properties of the highly nontrivial ‘‘flat’’ phase, that is critical and power-law rough. A complementary approach of Le Doussal and Radzihovsky[48] is via a solution of self-consistent integral equations (SCSA) that build on the large embedding $1/d_c$ expansion, with virtue of being exact in three limits: (i) $D \rightarrow 4$ (ϵ expansion) for arbitrary d_c , (ii) $d_c \rightarrow \infty$ ($1/d_c$ expansion) and (iii) $d_c = 0$ for arbitrary D , thereby providing best quantitative predictions, as judged by numerics and experiments.

The ‘‘flat’’ critical phase is characterized by *universal anomalous* elasticity with length scale-dependent elastic moduli

$$\kappa(q) \sim q^{-\eta}, \quad \mu(q) \sim \lambda(q) \sim q^{\eta_u}, \quad (75)$$

where for physical membranes $\eta \approx 0.82$ and the underlying embedding-space rotational invariance imposes exact relations [45–48],

$$\eta_u = 4 - D - 2\eta_\kappa, \quad \zeta = (4 - D - \eta)/2. \quad (76)$$

These indicate that at long scales, $q \rightarrow 0$, thermal fluctuations stiffen the effective bending modulus $\kappa(q)$ and soften membrane’s in-plane moduli, $\mu(q), \lambda(q)$.

Based on these, the SCSA[48] predicts a *universal* and *negative* Poisson ratio,

$$\lim_{q \rightarrow 0} \sigma \equiv \frac{\lambda(q)}{2\mu(q) + (D-1)\lambda(q)} = -\frac{1}{3}, \text{ for } D = 2, \quad (77)$$

that measures the ratio of in-plane compression of a membrane along an axis transverse to its strained direction. Its negative value indicates that such membrane actually expands transversely as it is being stretched. This approximate value of $-1/3$ compares extremely well with largest simulations[72] and higher order computations. This amazing fluctuation-driven anomalous elasticity phenomenology, uncovered using systematic Wilson-Fisher RG, can be understood qualitatively by playing around with a roughened piece of paper.

Finally I conclude by emphasizing that the universal anomalous elasticity is at the heart of stability of the 2D “flat” phase. To see this, observe that in contrast to the unstable Gaussian fixed point (describing fluctuations of a microscopic membrane), the “flat” *critical* phase at the AL fixed point, with a renormalized, momentum-dependent $\kappa(q)$, is characterized by root-mean-squared height undulations

$$h_{rms} = \sqrt{\langle h^2(\mathbf{x}) \rangle} = \left[\int_{L^{-1}} \frac{d^D q}{(2\pi)^d} \frac{T}{\kappa(q)q^4} \right]^{1/2} \sim L^\zeta, \quad (78)$$

with the roughness exponent $\zeta < 1$. Its best estimate for $D = 2, d = 3$ [48] is

$$\zeta = 0.59,$$

and has also been computed within ϵ and $1/d_c$ expansions[46–48, 73]. I note that despite unbounded power-law height undulations (78), the *rotational* $O(d)$ symmetry of the embedding space remains broken since $L^\zeta \ll L \rightarrow \infty$, despite two-dimensionality ($D = 2$) of the polymerized membrane field theory. It thus circumvents a naive application of the Hohenberg-Mermin-Wagner-Coleman theorem[57–59]. The rigorous form of the latter does not a priori apply to the higher-derivative polymerized membrane field theory, and thus does not forbid above findings, e.g., stability of the 2D flat phase. More physically, as can be seen from (78), theorem’s common heuristic application fails precisely because the state is controlled by a non-Gaussian fixed point with anomalous, momentum-dependent elastic moduli, specifically with $\eta > 0$. As a result $h_{rms}(L)/L \sim L^{-\eta/2} \rightarrow 0$ indicates that the “flat” phase is stabilized (for nonzero positive $\eta > 0$ generated by thermal fluctuations) by the very fluctuations that attempt to destabilize it, a phenomenon known as order-from-disorder.

Finally, I note that random heterogeneity also ubiquitously appears in most membrane realizations (see e.g., work on graphene[74]) and leads to a disorder-driven critical membrane phase, studied extensively starting with the work of Nelson and Radzihovsky[75, 76], with many that followed[71, 77, 78].

V. NEMATIC ELASTOMER

A final example of a critical phase that I will briefly discuss is a nematic elastomer, namely rubber – a randomly crosslinked polymer network composed of mesogenic groups, illustrated in Fig.9. It exhibits a spontaneous transition to a nematic phase, thereby driving an accompanying spontaneous uniaxial distortion of the elastic matrix, illustrated in Fig.9.[42]

Even in the absence of fluctuations, bulk nematic elastomers were predicted[79] and later observed to display an array of fascinating phenomena[42, 80], the most striking of which is the vanishing of stress for a range of strain, applied transversely to the spontaneous nematic axis. This striking softness is generic, stemming from the spontaneous orientational symmetry breaking by the nematic state, accompanied by the nemato-elastic Goldstone mode, that leads to the observed soft distortion and strain-induced director reorientation[79, 81], illustrated in Fig.10. This unique elastic phenomenon is captured even at the harmonic approximation of the fully nonlinear uniaxial Hamiltonian in Eq.(79),

$$\mathcal{H}_{elast} = \frac{1}{2} B_z w_{zz}^2 + \lambda_{z\perp} w_{zz} w_{\alpha\alpha} + \frac{1}{2} \lambda w_{\alpha\alpha}^2 + \mu w_{\alpha\beta}^2 + \frac{K}{2} (\nabla_\perp^2 u_z)^2, \quad (79)$$

where akin to earlier examples the components of the (rescaled) effective nonlinear strain tensor \underline{w} are given by

$$w_{zz} = \partial_z u_z + \frac{1}{2} (\nabla_\perp^2 u_z)^2, \quad (80)$$

$$w_{\alpha\beta} = \frac{1}{2} (\partial_\alpha u_\beta + \partial_\beta u_\alpha - \partial_\alpha u_z \partial_\beta u_z). \quad (81)$$

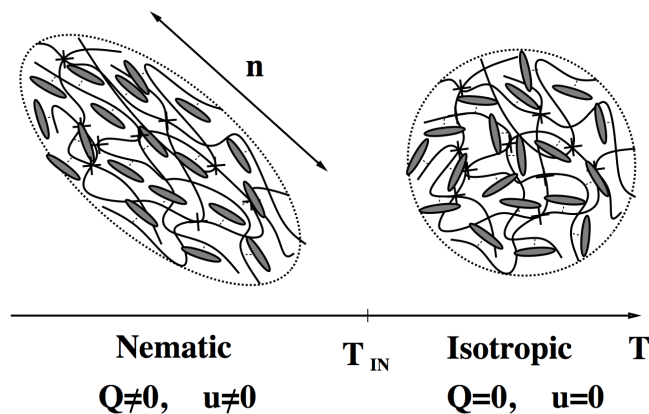


FIG. 9: Spontaneous uniaxial distortion of nematic elastomer driven through the isotropic-nematic transition.

The underlying rotational symmetry of the parent isotropic phase guarantees a vanishing of one of the five elastic constants[79, 81], $\mu_{\perp z}$ (i.e., the $w_{z\alpha}^2$ is missing from (79)), that usually characterizes harmonic deformations of a three-dimensional uniaxial solid[8], here with the uniaxial axis \hat{z} chosen spontaneously. Interestingly, examining (81), w_{zz} and $w_{\alpha\beta}$ have structure of, respectively, a uniaxially (e.g., smectic) and biaxially (e.g., columnar) periodic critical state. Thus, nematic elastomer is a three dimensional amorphous solid that is an amalgam of a smectic and columnar liquid crystals.

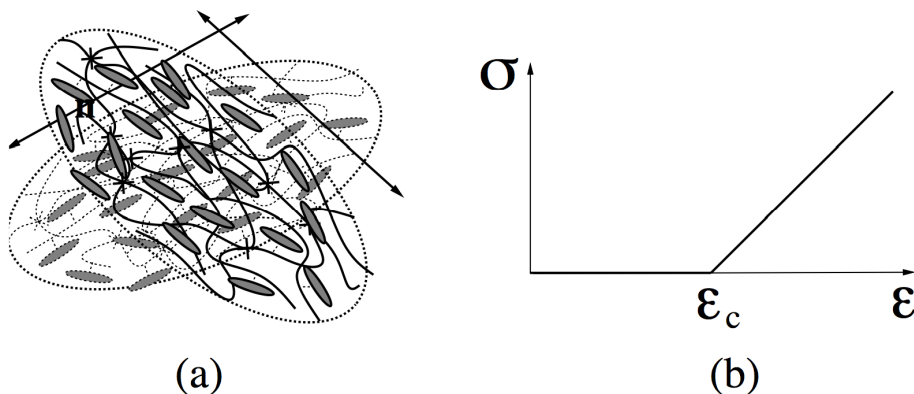


FIG. 10: (a) Simultaneous reorientation of the nematic director and of the uniaxial distortion is a low-energy nemato-elastic Goldstone mode of an ideal elastomer, that is responsible for its softness and (b) its resulting idealized flat (vanishing stress) stress-strain curve for a range of strains $0 < \varepsilon < \varepsilon_c$. [81]

Given this softness of the harmonic elasticity associated with symmetry-imposed vanishing of the $\mu_{z\perp}$ modulus, thermal and heterogeneity-driven fluctuations are divergent in 3d.[43, 82] Concomitantly, the elastic terms $(\nabla_{\perp} u_z)^2$ and $(\partial_z \mathbf{u}_{\perp})^2$ associated with transverse distortions are missing from the quadratic part of the elastic energy. Thus, as in other critical matter discussed in earlier sections, one expects qualitative importance of above elastic nonlinearities (81) in the presence of thermal fluctuations and network heterogeneity.[43, 82]

Similar to their effects in smectic, columnar liquid crystals, polymerized membranes, and other critical matter discussed earlier, in bulk elastomers thermal fluctuations (and network heterogeneity) leads to anomalous elasticity controlled by a tuning-free infrared attractive fixed point, with universal length-scale dependent elastic moduli, [43, 82]

$$K_{eff} \sim L^{\eta}, \quad \mu_{eff} \sim L^{-\eta_u}. \quad (82)$$

The resulting critical state can be shown[43] to be characterized by a universal non-Hookean stress-strain relation

$$\sigma_{zz} \sim (\varepsilon_{zz})^{\delta} \quad (83)$$

and a *negative* Poisson ratio for extension $\varepsilon_{xx} > 0$ transverse to the nematic axis

$$\varepsilon_{yy} = \frac{5}{7}\varepsilon_{xx}, \quad \varepsilon_{zz} = -\frac{12}{7}\varepsilon_{xx}. \quad (84)$$

While considerable progress has been made in understanding these fascinating materials, many questions, particularly associated with network heterogeneity remain open.

VI. SUMMARY AND CONCLUSIONS

In this chapter, I discussed a novel class of ordered states of matter that I dub “critical matter”. The common crucial feature of these exotic states is that, as a result of the underlying symmetry broken in the ordered state, a subset of elastic moduli of the associated Goldstone modes vanish identically. As a result, for sufficiently low dimensions, such system exhibit harmonic fluctuations that are divergent in the thermodynamic limit, and require treatment of Goldstone modes’ nonlinearities throughout the ordered phase (not just near a critical point). Treating these within renormalization group analysis, leads to an infrared stable fixed point that controls the resulting highly nontrivial, strongly interacting, and universal ordered state. The latter exhibits properties akin to that of a critical point, but extending over the entire phase, which I therefore naturally refer to as a “critical phase”.

As prominent examples of such systems, I have discussed smectics (with many soft and hard matter realizations, from paired superfluids (FFLO), spin-orbit coupled and frustrated bosons to quantum Hall stripes), cholesterics, helical magnets, columnar phases, putative spontaneous vortex lattices, polymerized membranes and nematic elastomers. While significant progress has been made in characterizing these systems, discovery of new systems (e.g., as quantum examples in physically accessible dimensions), understanding of effects of random heterogeneity and dynamics remain challenging open problems.

I finish by noting that there are also critical phases (many appearing as counter-parts of the ones discussed in this chapter), that I have not discussed here, where fluctuations are driven by quenched disorder, rather than by temperature or quantum fluctuations. These exhibit critical states of glassy Goldstone modes and generically appear in dimensions higher than their thermal counterparts[12–14, 39–41, 43, 71, 75–78, 83], and are thus of even stronger experimental relevance.

VII. ACKNOWLEDGMENTS

The material presented in these lectures is based on research done with a number of wonderful colleagues and friends, most notably David Nelson, John Toner, Pierre Le Doussal, Tom Lubensky, and Xiangjun Xing. I am indebted to them for much of my insight into the material presented here. This work was supported by the National Science Foundation through grants DMR-1001240 and DMR-0969083 as well by the Simons Investigator award from the Simons Foundation.

On a personal note, I have met and discussed physics with Michael Fisher at conferences, most often at the wonderful Rutgers Stat Mech meetings. I recall fondly Michael always sitting in a front row, sometimes flanked by Daniel and Matthew, strikingly paying close attention and asking probing questions even in the 3 mins student talks, and as attentively as in invited talks by distinguished senior faculty. I recall him always being kind and supportive in my own career. Although I have never had the pleasure of working with Michael, I have greatly benefited from his insight through his many seminal papers that influenced my own RG work (some described in this chapter). But perhaps more importantly, I indirectly learned physics from Michael through David Nelson, Daniel and Matthew, all of whom have strongly shaped my style, taste and approach to physics. And for that I am eternally grateful.

-
- [1] K. G. Wilson and M. E. Fisher, *Critical exponents in 3.99 dimensions*, Phys. Rev. Lett. **28** (4), 240-243 (1972).
 - [2] M. E. Fisher, *The renormalization group in the theory of critical behavior*. Reviews of Modern Physics, **46**(4), 597 (1974).
 - [3] K. G. Wilson and J. Kogut, *The renormalization group and the ϵ expansion*, Physics Reports **12**, 78 - 199 (1974).
 - [4] P. Chaikin and T.C. Lubensky, *Principles of Condensed Matter Physics*, Cambridge University Press, Cambridge 1995.
 - [5] Jean Zinn-Justin, *Quantum Field Theory and Critical Phenomena* (International Series of Monographs on Physics) 5th Edition.
 - [6] In quantum phase transitions, temperature T introduces a finite size cutoff $\hbar/k_B T$ into the imaginary time. As a result critical behavior can be probed even in a fan of $\delta g(T)$ away from a quantum critical point.[7]
 - [7] S. Sachdev, *Quantum Phase Transitions*, Cambridge University Press, 1999.

- [8] L. D. Landau, in *Collected papers of L. D. Landau*, edited by D. ter Haar (Gordon and Breach, New York, 1965), p. 209; L. D. Landau and E. M. Lifshitz, *Statistical Physics* (Pergamon, London, 1969).
- [9] A generalized m -Lifshitz model, has elasticity with m “soft” (Laplacian) axes and $d - m$ complementary “hard” (gradient) axes. In this nomenclature, the conventional classical 3d smectic is the $m = 2$ -Lifshitz model, and 2+1d quantum smectic and 3d classical columnar liquid crystal are described by the $m = 1$ -Lifshitz model. Other generalizations include a nonscalar Goldstone-mode field as in e.g., tethered membranes[44, 68, 69, 71] and nematic elastomers[43]
- [10] P. de Gennes and J. Prost, *The Physics of Liquid Crystals* (Clarendon Press, Oxford, 1993).
- [11] G. Grinstein and R. A. Pelcovits, Phys. Rev. Lett. **47**, 856 (1981).
- [12] L. Radzihovsky, J. Toner, *Nematic-to-smectic-A transition in aerogel*, Phys. Rev. Lett. **79**, 4214 (1997).
- [13] L. Radzihovsky, J. Toner, *Smectic liquid crystals in random environments*, Phys. Rev. B **60**, 206 (1999).
- [14] T. Bellini, L. Radzihovsky, J. Toner, N. A. Clark, *Universality and scaling in the disordering of a smectic liquid crystal*, Science **204**, 5544 (2001).
- [15] Matthew A. Glaser, Gregory M. Grason, Randall D. Kamien, A. Kosmrlj, Christian D. Santangelo, P. Zihlerl, *Soft spheres nake more mesophases*, Europhys. Lett. **78**, 46004 (2007).
- [16] M. P. Lilly, K. B. Cooper, J. P. Eisenstein, L. N. Pfeiffer, and K. W. West, *Evidence for an anisotropic state of two-dimensional electrons in high Landau levels*, Phys. Rev. Lett. **82**, 394 (1999).
- [17] R. R. Du, D.C. Tsui, H.L. Stormer, L.N. Pfeiffer, K.W. Baldwin, K.W. West, *Strongly anisotropic transport in higher two-dimensional Landau levels*, Solid State Comm. **109**, 389 (1999).
- [18] A. A. Koulakov, M. M. Fogler, and B. I. Shklovskii, *Charge density wave in two-dimensional electron liquid in weak magnetic field*, Phys. Rev. Lett. **76**, 499 (1996).
- [19] R. Moessner and J. T. Chalker, *Exact results for interacting electrons in high Landau levels*, Phys. Rev. B **54**, 5006 (1996).
- [20] E. Fradkin and S.A. Kivelson, *Liquid-crystal phases of quantum Hall systems*, Phys. Rev. B **59**, 8065 (1999).
- [21] A. H. MacDonald and M. P. A. Fisher, *Quantum theory of quantum Hall smectics*, Phys. Rev. B **61**, 5724 (2000).
- [22] L. Radzihovsky, A. T. Dorsey, *Theory of Quantum Hall Nematics*, Phys. Rev. Lett. **88**, 216802 (2002).
- [23] P. Fulde and R.A. Ferrell, *Superconductivity in a Strong Spin-Exchange Field*, Phys. Rev. **135**, A550 (1964).
- [24] A.I. Larkin and Yu. N. Ovchinnikov, *Nonuniform state of superconductors*, Sov. Phys. JETP **20**, 762 (1965).
- [25] L. Radzihovsky and A. Vishwanath, *Quantum liquid crystals in an imbalanced Fermi gas: fluctuations and fractional vortices in Larkin-Ovchinnikov states*, Phys. Rev. Lett. **103**, 010404 (2009); L. Radzihovsky, *Fluctuations and phase transitions in Larkin-Ovchinnikov liquid-crystal states of a population-imbalanced resonant Fermi gas*, Phys. Rev. A **84**, 023611 (2011); L. Radzihovsky, *Quantum liquid-crystal order in resonant atomic gases* (invited review) *Physica C* **481**, 189-206 (2012).
- [26] Leo Radzihovsky, Daniel E. Sheehy, *Imbalanced Feshbach-resonant Fermi gases*, Rep. Prog. Phys. **73**, 076501 (2010).
- [27] D. F. Agterberg, J. S. Davis, S. D. Edkins, E. Fradkin, D. J. Van Harlingen, S. A. Kivelson, P. A. Lee, L. Radzihovsky, J. M. Tranquada, and Y. Wang, *The physics of pair-density waves: cuprate superconductors and beyond*, Annu. Rev. Condens. Matter Phys. **11**, 231 (2020).
- [28] L. Radzihovsky and S. Choi, *P-wave resonant Bose gas: a finite-momentum spinor superfluid*, Phys. Rev. Lett. **103**, 095302 (2009); Phys. Rev. A **84**, 043612 (2011).
- [29] Hui Zhai, *Degenerate quantum gases with spin-orbit coupling: a review*, Rep. Prog. Phys. **78**, 026001 (2015).
- [30] Tzu-Chi Hsieh, Han Ma, Leo Radzihovsky, *Helical superfluid in a frustrated honeycomb Bose-Hubbard model*, Phys. Rev. A **106**, 023321 (2022).
- [31] T. C. Lubensky, *Low-Temperature Phase of Infinite Cholesterics*, Phys. Rev. Lett. **29**, 206 (1972).
- [32] L. Radzihovsky, T. C. Lubensky, *Nonlinear smectic elasticity of helical state in cholesteric liquid crystals and helimagnets*, Phys. Rev. E **83**, 051701 (2011).
- [33] S. Muhlbauer, B. Binz, F. Jonietz, C. Peiderer, A. Rosch, A. Neubauer, R. Georgii, and P. Boni, “Skyrmion lattice in a chiral magnet”, Science **323**, 915 (2009).
- [34] Doron Bergman, Jason Alicea, Emanuel Gull, Simon Trebst, Leon Balents, *Order by disorder and spiral spin liquid in frustrated diamond lattice antiferromagnets*, Nature Physics **3**, 487 (2007).
- [35] A. Mulder, R. Ganesh, L. Capriotti, and A. Paramekanti, *Spiral order by disorder and lattice nematic order in a frustrated Heisenberg antiferromagnet on the honeycomb lattice*, Phys. Rev. B **81**, 214419 (2010).
- [36] P. Canfield, P. Gammel, D. Bishop, *New magnetic superconductors: a toy box for solid-state physicists*, Physics Today, October (1998).
- [37] U. Yaron, P.L. Gammel, A.P. Ramirez, D.A. Huse, D.J. Bishop, A.I. Goldman, C. Stassis, P.C. Canfield, K. Mortensen and M.R. Eskildsen, *Microscopic coexistence of magnetism and superconductivity in $ErNi_2B_2C$* , Nature, **386**, 236 (1996).
- [38] H. S. Greenside, E. I. Blount and C.M. Varma, *Possible coexisting superconducting and magnetic states*, Phys. Rev. Lett. **46**, 49 (1981); E. I. Blount and C.M. Varma, *ibid* **42**, 1079 (1979); T.K. Ng and C.M. Varma, *ibid.* **78**, 330, *ibid.*, 3745 (1997).
- [39] K. Saunders, L. Radzihovsky, and J. Toner, *A discotic disguised as a smectic: a hybrid columnar bragg glass*, Phys. Rev. Lett. **85**, 4309 (2000).
- [40] A. M. Ettouhami, Karl Saunders, L. Radzihovsky, John Toner, ‘Soft’ anharmonic vortex glass in ferromagnetic superconductors, Phys. Rev. Lett. **87**, (2001) 27001.
- [41] A. M. Ettouhami, Karl Saunders, L. Radzihovsky, John Toner, *Elasticity, fluctuations and vortex pinning in ferromagnetic superconductors: A columnar elastic glass*, Phys. Rev. B **71**, 224506 (2005).
- [42] M. Warner, E.M. Terentjev, *Liquid Crystal Elastomers*, Oxford University Press, 2003.
- [43] X. Xing and L. Radzihovsky, *Thermal fluctuations and anomalous elasticity of homogeneous nematic elastomers*, Europhys. Lett. **61**, 769 (2003); *Nonlinear elasticity, fluctuations and heterogeneity of nematic elastomers*, Annals of Physics **323** 105-

- 203 (2008). *Universal elasticity and fluctuations of nematic gels*, Phys. Rev. Lett. **90**, 168301 (2003).
- [44] For a review, and extensive references, see the articles in *Statistical Mechanics of Membranes and Interfaces*, 2nd edition, Jerusalem Winter School, edited by D. R. Nelson, T. Piran, and S. Weinberg (World Scientific, Singapore, 1989).
- [45] D. R. Nelson and L. Peliti, *Fluctuations in membranes with crystalline and hexatic order*, J. Phys. (Paris) **48**, 1085 (1987).
- [46] J. A. Aronovitz and T. C. Lubensky, Fluctuations of solid membranes, Phys. Rev. Lett. **60**, 2634 (1988); J. A. Aronovitz, L. Golubovic, and T. C. Lubensky, *Fluctuations and lower critical dimensions of crystalline membranes*, J. Phys.(Paris) **50**, 609 (1989).
- [47] F. David and E. Guitter, *Crumpling transition in elastic membranes: renormalization group treatment*, Europhys. Lett. **5**, 709 (1988).
- [48] P. Le Doussal and L. Radzihovsky, *Self-consistent theory of polymerized membranes*, Phys. Rev. Lett. **69**, 1209 (1992).
- [49] L. Radzihovsky, *Statistical mechanics and geometry of random manifolds*, Ph. D. Thesis, Harvard University, (1993).
- [50] Another, distinct class of “self-organized” critical phases have been proposed in Per Bak, Chao Tang, and Kurt Wiesenfeld, *Self-organized criticality: An explanation of the 1/f noise*, Phys. Rev. Lett. **59** 381, (1987). We will not discuss such nonequilibrium dynamical systems.
- [51] James McIver, Monika Aidelsburger, Martin Claassen, *Floquet engineering of quantum materials*, Nature Commun. Phys., Focus, 17 March 2022.
- [52] Daniel E. Sheehy, Leo Radzihovsky, *BEC-BCS crossover in “magnetized” Feshbach-resonantly paired superfluids*, Phys. Rev. Lett. **96**, 060401 (2006).
- [53] Daniel E. Sheehy, Leo Radzihovsky, *BEC-BCS crossover, phase transitions and phase separation in polarized resonantly paired superfluids*, Annals of Physics **322**, 1790 (2007).
- [54] M. C. Revelle, J. A. Fry, B. A. Olsen B A, R. G. Hulet, *1D to 3D Crossover of a Spin-Imbalanced Fermi Gas*, Phys. Rev. Lett. **117** 235301 (2016).
- [55] A. Caillé, *Remarks on the scattering of x-rays by A-type smectics*, C. R. Acad. Sci. Ser. B **274**, 891 (1972).
- [56] R. E. Peierls, Helv. Phys. Acta Suppl. **7**, 81 (1934).
- [57] P.C. Hohenberg, *Existence of long-range order in one and two dimensions*, Phys. Rev. **158**, 383 (1967).
- [58] N.D. Mermin, H. Wagner, *Absence of ferromagnetism or antiferromagnetism in one- or two-dimensional isotropic heisenberg models*, Phys. Rev. Lett. **17**, 1133 (1966).
- [59] S. Coleman, *There are no Goldstone bosons in two dimensions*, Commun. Math. Phys. **31**, 259 (1973).
- [60] F. Lindemann, *About the calculation of molecular own frequencies*, Z.Phys, **11**, 609 (1910).
- [61] J. Toner and D. R. Nelson, *Smectic, cholesteric, and Rayleigh-Benard order in two dimensions*, Phys. Rev. B **23**, 316 (1981).
- [62] J. Als-Nielsen, J. D. Litster, R. J. Brigeneau, M. Kaplan, C. R. Safinya, A. Lindegaard-Andersen, and S. Mathiesen, *Observation of algebraic decay of positional order in a smectic liquid crystal*, Phys. Rev. B **22**, 312 (1980).
- [63] L. Golubovic, Z. Wang, *Anharmonic elasticity of smectics A and the Kardar-Parisi-Zhang model*, Phys. Rev. Lett. **69** 2535 (1992).
- [64] Mehran Kardar, Giorgio Parisi, and Yi-Cheng Zhang, *Dynamic scaling of growing interfaces* , Phys. Rev. Lett. **56**, 889 (1986).
- [65] A.I. Larkin, D.E. Khmel’nitskii, *Phase transition in uniaxial ferroelectrics*, Zh. Eksp. Teor. Fiz **56**, 2087 (1969),
- [66] M. E. Fisher, S. K. Ma, B. G. Nickel, *Critical exponents for long-range interactions*, Phys. Rev. Lett. **29**, 917 (1972).
- [67] Geim A. K. , Novoselov K. S. , *The rise of graphene*, Nat. Mater. **6**, 183-191 (2007).
- [68] Leo Radzihovsky and John Toner, *A new phase of tethered membranes: Tubules* Phys. Rev. Lett. **75**, 4752 (1995).
- [69] Leo Radzihovsky, John Toner, *Elasticity, shape fluctuations and phase transitions in the new tubule phase of anisotropic tethered membranes*, Phys.Rev.E **57**:1832-1863 (1998).
- [70] Mark Bowick, Marco Falcioni, and Gudmar Thorleifsson, *Numerical observation of a tubular phase in anisotropic membranes*, Phys. Rev. Lett. **79**, 885 (1997).
- [71] Pierre Le Doussal, Leo Radzihovsky, *Anomalous elasticity, fluctuations and disorder in elastic membranes*, Annals of Physics **392**, 340-410 (2018).
- [72] M. Falcioni, M. Bowick, E. Guitter, and G. Thorleifsson, *The Poisson ratio of crystalline surfaces*, Europhys. Lett. **38**, 67 (1997).
- [73] O. Coquand, D. Mouhanna, S. Teber, *Flat phase of polymerized membranes at two-loop order*, Phys.Rev. E **101**, 062104 (2020).
- [74] P. Y. Huang, et al., *Grains and grain boundaries in single-layer graphene atomic patchwork quilts*, Nature **469**, 389 (2011).
- [75] D. R. Nelson and L. Radzihovsky, *Polymerized membranes with quenched random internal disorder*, Europhys. Lett., **16**, 79 (1991).
- [76] L. Radzihovsky and D. R. Nelson, *Statistical mechanics of randomly polymerized membranes*, Phys. Rev. A, **44**, 3525 (1991).
- [77] D. C. Morse and T. C. Lubensky, *Curvature disorder in tethered membranes: A new flat phase at T=0.*, Phys. Rev. A **46**, 1751 (1992).. D. C. Morse, T. C. Lubensky, and G. S. Grest, *Quenched disorder in tethered membranes*, Phys. Rev. A **45**, R2151 (1992).
- [78] Le Doussal and L. Radzihovsky, *Flat glassy phases and wrinkling of polymerized membranes with long range disorder*, Phys. Rev. B, **R48**, 3548 (1993).
- [79] L. Golubovic and T. C. Lubensky, *Nonlinear elasticity of amorphous solids*, Phys. Rev. Lett. **63**, 1082 (1989).
- [80] M. Warner and E. M. Terentjev, *Nematic elastomers—a new state of matter?*, Prog. Polym. Sci. **21**, 853(1996), and references therein; E. M. Terentjev, *Liquid-crystalline elastomers*, J. Phys. Cond. Mat. **11**, R239(1999).
- [81] T. C. Lubensky, R. Mukhopadhyay, L. Radzihovsky, X. Xing, *Symmetries and elasticity of nematic gels*, Phys. Rev. E **66**,

011702 (2002).

- [82] O. Stenull and T.C. Lubensky, *Phase transitions and soft elasticity of smectic elastomers*, Europhys. Lett. **61**, 779 (2003).
- [83] Pierre Le Doussal, Leo Radzihovsky, *Thermal buckling transition of crystalline membranes in a field*, Phys. Rev. Lett. **127**, 015702 (2021).